



L-2010-215
10 CFR 52.3

September 22, 2010

U.S. Nuclear Regulatory Commission
Attn: Document Control Desk
Washington, D.C. 20555-0001

Re: Florida Power & Light Company
Proposed Turkey Point Units 6 and 7
Docket Nos. 52-040 and 52-041
Supplemental Response to Request for Additional Information Letter No. 004
Standard Review Plan Section 02.04.06 – Probable Maximum
Tsunami Flooding -Question No. 02.04.06-2 (eRAI 4809)

References:

1. NRC Letter to FPL dated August 3, 2010, Request for Additional Information Letter No. 004 Related to SRP Section 02.04.06 - Probable Maximum Tsunami Floodings for the Turkey Point Nuclear Plant Units 6 and 7 Combined License Application (ML102150446)
2. FPL Letter L-2010-195 to NRC dated September 2, 2010, Response to Request for Additional Information Letter No. 004 (eRAI 4809) Standard Review Plan Section 02.04.06 - Probable Maximum Tsunami Flooding

Florida Power & Light Company (FPL) provides, as an attachment to this letter, its response to Question No. 02.04.06-2 in the Nuclear Regulatory Commission's (NRC) request for additional information provided in Reference 1 (eRAI 4809). The partial response to eRAI 4809 (Question Nos. 02.04.06-1 and 02.04.06-3) was provided by Reference 2. The attachment identifies changes that will be made in a future revision of the Turkey Point Units 6 and 7 Combined License Application (if applicable).

If you have any questions, or need additional information, please contact me at 561-691-7490.

I declare under penalty of perjury that the foregoing is true and correct.

Executed on September 22, 2010

Sincerely,

William Maher
Senior Licensing Director – New Nuclear Projects

Attachment: FPL Response to NRC RAI No. 02.04.06-2 (eRAI 4809)

cc:

PTN 6 & 7 Project Manager, AP1000 Projects Branch 1, USNRC DNRL/NRO
Regional Administrator, Region II, USNRC
Senior Resident Inspector, USNRC, Turkey Point Plant 3 & 4

Florida Power & Light Company

700 Universe Boulevard, Juno Beach, FL 33408

DD97
NRO

Proposed Turkey Point Units 6 and 7
Docket Nos. 52-040 and 52-041
L-2010-215 Attachment Page 1 of 48

NRC RAI Letter No.: PTN-RAI-LTR-004

SRP Section: FSAR 02.04.06, Probable Maximum Tsunami Hazards

NRC RAI Number: 02.04.06-2 (eRAI 4809)

Section C.I.2.4.6.4 of Regulatory Guide 1.206 (RG 1.206) provides specific guidance with respect to tsunami analysis. This includes providing a complete description of the analysis procedure used to calculate tsunami wave height and period at the site, including the theoretical bases of the models, their verification and the conservatism of all input parameters.

Provide a complete description in the updated FSAR of the numerical modeling methodology used for the revised tsunami analysis and supply water level results specific to the site, taking into account the regional and local (site-specific) bathymetry/topography.

FPL RESPONSE:

A computer model is developed to simulate tsunami propagation and establish the probable maximum tsunami flood elevation at the Turkey Point Units 6 & 7 site. FSAR Section 2.4.6 established that the probable maximum tsunami (PMT) would likely be generated by an earthquake in the Azores-Gibraltar fracture zone. Tsunami generation at the source as presented in Mader (2001) is considered to envelope the PMT water level at the site and is adopted in this analysis.

Delft3D-FLOW module of the Delft3D modeling system is used to simulate tsunami wave propagation and run-up at Units 6 & 7. The FLOOD solution scheme is used to solve the governing equations on a depth-averaged domain. The FLOOD scheme is developed for rapidly varying flows and rapid flooding and drying of lands (Stelling and Duinmeijer, 2003), and therefore applicable for simulating tsunami wave modification and run-up.

Details of the model and proposed revision to the FSAR Subsection 2.4.6 are provided below.

References:

Mader, C.M., "Modeling the 1755 Lisbon Tsunami", *Science of Tsunami Hazards*, Volume 19, No. 2, pp. 93-99, 2001.

Stelling, G.S. and Duinmeijer, S.P.A., "A staggered conservative scheme for every Froude number in rapidly varied shallow water flows", *International Journal for Numerical Methods in Fluids*, Volume 43, pp. 1329-1354, 2003.

This response is PLANT SPECIFIC.

ASSOCIATED COLA REVISIONS:

The first paragraph in Subsection 2.4.6 will be updated in a future revision as indicated below:

This subsection examines the tsunamigenic sources and identifies the probable maximum tsunami (PMT) that could affect the safety-related facilities of Units 6 & 7. It evaluates potential tsunamigenic source mechanisms, source parameters, and **resulting** tsunami propagation from published studies, and ~~provides information on~~ **estimates** tsunami water levels ~~expected at the site~~ **based on site-specific numerical model simulation results**. Historical tsunami events recorded along the Florida coast are reviewed to support the PMT assessment. The approach taken is aligned with the PMT evaluation methodology proposed in NUREG/CR-6966 (Reference 201).

The first paragraph in Subsection 2.4.6.1 will be updated in a future revision as indicated below:

The Atlantic and Gulf of Mexico Tsunami Hazards Assessment Group (AGMTHAG) evaluated potential tsunamigenic source mechanisms that may generate destructive tsunamis and affect the U.S. Atlantic and Gulf of Mexico coasts (Reference 202). The major tsunamigenic sources that may affect the southeastern U.S. coasts can be summarized as follows: submarine landslides along the U.S. Atlantic margin, submarine landslides in the Gulf of Mexico, farfield submarine landslide sources, earthquakes in the Azores-Gibraltar plate boundary, and earthquakes in the north Caribbean subduction zones (referred to as the Caribbean-North American plate boundary in Subsection 2.5.1-1.4).

Subsection 2.4.6.1.1 will be updated in a future revision as indicated below:

Submarine landslide zones along the U.S. Atlantic margin are concentrated along the New England and Long Island, New York sections of the margin, outward of major ancient rivers in the mid-Atlantic region, and in the salt dome province offshore of North **and South Carolina Carolinas**, as shown in Figure 2.4.6-201 (Reference 202). Although submarine landslides along the U.S. Atlantic margin, from Georges Bank offshore of the New England coast to Blake Spur south of the Carolina Trough, have the potential to cause devastating tsunamis locally, the presence of a wide continental shelf is expected to reduce their impact at the shoreline **near the landslides** (Reference 202).

Units 6 & 7 are located approximately 400 miles (640 kilometers) southwest of Blake Spur with a wide ~~and shallow~~ continental **slope and shelf** in between (Figure 2.4.6-201). **Details of the Atlantic continental slope and shelf near the site are described in Subsection 2.5.1.1.1.1.** Additionally, the landslide zones are oriented so that Units 6 & 7 would be away from the main axis of submarine landslide-generated tsunamis. Consequently, the impact of any submarine landslide-generated tsunami

~~in~~ **on** the continental **slope and** shelf north of Blake Spur would be considerably reduced before reaching Units 6 & 7.

Twichell et al. identified three morphologic provinces along the Blake Escarpment with varying erosional behavior (Reference 203). These are (1) valleys with tributary gullies, (2) box canyons, and (3) strait terraces. Valleys with tributary gullies are in the northern part of the escarpment near Blake Spur that have undergone no or very little erosion over time. Box canyons are formed by the differential settlement of base rock probably over a long period and are identified south of the Jacksonville fracture zone. The overlying carbonate strata in box canyons are fragmented with continued erosion. The middle reach of the escarpment has straight terraces formed by differential erosion of lithologic differences in the strata exposed along the cliff faces and has lower erosion potential than box canyons (Reference 203). The study by Twichell et al. identified evidence of debris accumulation at the base of the escarpment; however, it did not characterize any tsunamigenic source in the escarpment (Reference 203). Units 6 & 7 are sheltered by the islands of the Bahamas from tsunamis, if any, generated in the region, thus protecting Units 6 & 7 from being affected by large tsunamis.

The Ocean Drilling Program (ODP) provides stratigraphic information on the Bahamas platform and the Straits of Florida from borehole and seismic reflection survey results. The ODP data suggest evidence of significant submarine debris flows and turbidite deposits during a four million year interval in the middle Miocene (Reference 217). However, no stratigraphic evidence could be established to relate these Miocene gravity flows to any tsunami deposit or tsunami-like event along the southern Florida coasts. After the Miocene, no debris flow or turbidite deposit could be identified in this region, possibly due to the erosional effects of the Gulf Loop Current that was first established in the Pliocene. It is hypothesized that the debris flow and turbidite deposit resulted from materials that had accumulated atop the carbonate banks at a marine high stand, which became unstable as sea level fell (Reference 217). Such debris flows are not expected to occur in the recent geological environment of eustatic sea level rise. Therefore, submarine landslide in the Straits of Florida and Bahamas regions is precluded as a PMT source candidate for the Units 6 & 7 site. Details of stratigraphic information in the Bahamas and the Straits of Florida are provided in Subsection 2.5.1.1.2. Potential geological hazards near the site region are described in Subsection 2.5.1.1.5.

Information on submarine landslide along the northern coast of Cuba is very scarce. Iturralde-Vinent (Reference 218) summarizes the current understanding of tsunami hazards in Cuba, details of which are provided in Subsection 2.5.1.1.5. Iturralde-Vinent identifies potential tsunami hazards for the Cuban north coast region based on large carbonate boulders found on marine terraces; however, no

submarine landslide zones were identified in this region. Consequently, a submarine landslide along the north coast of Cuba was not included as a candidate PMT source for the Units 6 & 7 site.

Units 6 & 7, therefore, would not be impacted by significant submarine landslide generated tsunamis from the U.S. Atlantic margin, **the Straits of Florida, Bahamas, or Cuba region.**

The first paragraph of Subsection 2.4.6.1.5 will be updated in a future revision as indicated below:

The Caribbean region is characterized by high seismic activities and is associated with a large number of past tsunamis (References 210 and 211). Tsunami sources in the northeastern Caribbean Basin that may affect the Florida Atlantic coast include the Puerto Rico and Hispaniola trenches, as shown in Figure 2.4.6-207. AGMTHAG simulated the distribution of peak offshore tsunami amplitude along the Gulf of Mexico and Atlantic Coasts from a postulated earthquake in the Puerto Rico trench. The simulation, which used a linear long-wave model for the deepwater regions and did not include frictional effects, predicted the maximum tsunami amplitude to be no more than 0.1 meter (0.3 foot) at a water depth of 250 meters (820 feet) near the longitude of approximately 80.2° W (longitude position estimated from Figure 8-2c of Reference 202). This longitude position represents generally the location within the Straits of Florida, which is south-southwest of Units 6 & 7. The maximum deepwater tsunami amplitudes along the U.S. Atlantic coast, however, were much higher, close to 5 meters (16.4 feet) near latitude 40° N (latitude position represents generally a location offshore of the New York/New Jersey coast) and approximately 3 meters (10 feet) near latitude 33.2° N (offshore of the South Carolina coast). The model simulated a maximum deepwater tsunami amplitude of about 3.5 meters (11.5 feet) near 28° N (offshore of Palm Bay, Florida) (Figure 8-3c of Reference 202). The relatively small tsunami amplitude near Units 6 & 7 is primarily a result of the presence of the Bahamas **Bahama** platform to the east, as shown in Figure 2.4.6-208. AGMTHAG did not model the propagation of tsunami waves across the continental shelf (water depth less than 250 meters or 820 feet) and run-up (Reference 202).

Subsection 2.4.6.1.6 will be updated in a future revision as indicated below:

A significant tsunami generated directly by an earthquake only occurs if the earthquake is large (magnitude, with few exceptions, greater than about 6.5) and if the fault slip associated with the earthquake has a significant vertical component of offset **seafloor displacement** (thrust or normal **faults**) ~~the extends to the seafloor~~. There is no record of surface fault ~~offset~~ **rupture and significant seismic displacement at the seafloor** associated with any historical earthquake in the central and eastern United States including the 1886 Charleston, South Carolina event of about magnitude 7, the largest historical earthquake in the U.S. Atlantic coastal region. Therefore **Consequently**, the conditions for

tsunamigenesis by ~~submarine fault~~ **seafloor** displacement associated with an earthquake do not appear to exist along the U.S. Atlantic margin, ~~and~~. Units 6 & 7, therefore, would not be impacted by significant **tsunamis as a result of vertical seafloor displacement** ~~submarine fault offset~~ generated ~~tsunamis~~ associated with the U.S. Atlantic margin earthquakes.

Although the north Caribbean subduction zone is noted for several seismically-generated tsunamis in recent times, as described in Subsection 2.4.6.1.5, potential submarine landslides of the carbonate platform edge north of Puerto Rico are capable of producing large tsunamis locally (see Subsection 2.4.6.2 and 2.5.1.1.5 for detailed discussions). However, because the Units 6 & 7 site is sheltered by the Bahamas Islands, such landslide-generated tsunamis are not expected to affect the site. Therefore, a landslide in the carbonate platform north of Puerto Rico is not considered as a PMT source for the Units 6 & 7 site.

Subsection 2.4.6.1.7 will be updated in a future revision as indicated below:

Units 6 & 7 are not located in the immediate vicinity of any tsunamigenic source. The landslide zone nearest to Units 6 & 7 is located on the west Florida slopes within the Gulf of Mexico, separated by a very wide and shallow continental shelf and the entire width of the Florida peninsula. There is no historical evidence of any tsunami from landslides in the Gulf of Mexico. Landslides in the U.S. Atlantic margin may potentially generate local destructive tsunamis. However, because Units 6 & 7 are located far away from any such sources, is mostly sheltered by the Bahamas platform, and is protected by a retaining wall structure with top elevation of 20.0 feet to 21.5 feet NAVD 88, such tsunamis are not expected to cause any flooding concern to the safety-related facilities of Units 6 & 7. The orientation of the Puerto Rico trench and the presence of the ~~Bahamas~~**Bahama** platform prevents any destructive tsunami to impact Units 6 & 7 from this source. Therefore, it is concluded that the PMT would likely be caused by earthquake-generated transoceanic tsunamis from the Azores-Gibraltar plate boundary. Characteristics of tsunami source generators for both Azores-Gibraltar plate boundary and Caribbean region are presented in Subsection 2.4.6.3.

The last paragraph of Subsection 2.4.6.2 will be updated in a future revision as indicated below:

Lockridge et al. reported tsunamis and tsunami-like events in the U.S. east coast in addition to the events reported in the NGDC database (**Reference 208**). Most of these additional events originated along the New York, New Jersey, and Delaware coasts, and the Florida Atlantic coast remained unaffected. ~~An extensive literature search did not reveal any evidence of seismic paleotsunami deposit in the region.~~ **No seismically-induced paleotsunami deposits have been positively identified in available scientific literature within the 200-mile radius of the Turkey Point site, as described in Subsection 2.5.1.1.5. Distinguishing characteristics of tsunami versus storm deposits are also**

described in Subsection 2.5.1.1.5. Turkey Point site boring log data interpretation and relevance to paleotsunami deposits is described in Subsection 2.5.1.2.2.

Subsection 2.4.6.3 will be updated in a future revision as indicated below:

There is no tsunamigenic source present in the immediate vicinity of Units 6 & 7. The submarine landslide zones in the U.S. Atlantic margin and along the Gulf of Mexico coast are located far away from Units 6 & 7 and are separated by a wide and shallow continental **slope and** shelf, which would reduce the impact of any landslide-generated tsunamis at Units 6 & 7. The north Caribbean subduction zone and Azores-Gibraltar plate boundary are identified as the primary tsunamigenic earthquake sources that could affect the site. Model simulation results indicate that the shallow-Bahamas **Bahama** platform shields Units 6 & 7 from tsunamis generated in the northern Caribbean region (Reference 211). Therefore, the PMT for Units 6 & 7 would likely be transoceanic tsunamis from the Azores-Gibraltar region. The most recent major earthquake in the region occurred in 1969 (Mw = 7.8) and generated a small tsunami amplitude locally (Reference 202).

Subsections 2.4.6.4 and 2.4.6.5 will be updated in a future revision as indicated below:

The maximum tsunami water level at **Units 6 & 7 is obtained for the postulated PMT generated by earthquake in the Azores-Gibraltar fracture zone. Tsunami propagation and the effects of near shore bathymetric variation at the Florida Atlantic coast are simulated in a two-dimensional computer model**, based on the results of published tsunami studies **the development of which** is summarized in the following subsections. Detailed water level records near Units 6 & 7 are not available for tsunamis generated by past earthquakes in the Azores-Gibraltar fracture zone or in the Caribbean subduction zone for the listed earthquake magnitudes. **In order to establish the model boundary condition, the resulting water levels in deep waters in the computer simulations by Mader (Reference 202) and Knight (Reference 211) for tsunamis generated from the Azores-Gibraltar and Caribbean sources are used as guidance for the PMT model.** However, tsunami water levels at Units 6 & 7 are evaluated based on the results of computer simulations from the two sources (Atlantic and Caribbean regions) with larger earthquake magnitudes compared to those described in Subsection 2.4.6.3. Thus, detailed modeling analysis of tsunami amplitude and its propagation is not performed. This qualitative approach is considered adequate in assessing the PMT hazards at Units 6 & 7 because the tsunamigenic earthquake magnitudes adopted in the reference studies are more severe than any recorded earthquake in the two source regions. **The PMT simulation for Units 6 & 7 uses the computer code Delft3D-Flow, which is a multi-dimensional modeling system that is capable of simulating the hydrodynamics and transport processes for fluvial, estuarine, and coastal environments (Reference 219).**

2.4.6.4.1 Numerical Modeling Approach and Conceptualization

Subsection 2.4.6.1 establishes the Azores-Gibraltar fracture zone (specifically the 1755 Lisbon Earthquake source) as the candidate PMT source for Units 6 & 7. It is postulated that the earthquake-generated transoceanic tsunami from this source would propagate across the Atlantic Ocean and would be modified at the Bahama platform before reaching the site. Tsunami generation and transoceanic propagation from this source were studied previously using numerical model simulations (References 202 and 209). However, tsunami wave modification on the shallow Bahama platform and wave run-up onshore near Units 6 & 7 have not been reported in any literature. The primary objectives in developing the numerical model for Units 6 & 7 therefore are to account for the effects of near shore bathymetric variation on tsunami wave modification and tsunami run-up onshore.

Delft3D-FLOW, the flow module of the Delft3D modeling system, simulates two- or three-dimensional unsteady flow problems from tide or meteorological forcing. The FLOW module provides hydrodynamic solutions for which the horizontal length and time scales are significantly larger than the vertical scales (Reference 219) representing the shallow water conditions. Delft3D-FLOW has the capability of invoking the FLOOD solver, which employs a numerical technique (Reference 220) that can be applied to problems involving rapidly varied flows, for example, in hydraulic jumps and bores, and sudden flow transitions including rapid flooding and drying of land. The FLOOD scheme is suitable for simulating the tsunami waves, embankment breaches, hydraulic jumps, and flows over obstructions (Reference 219). Consequently, in the present analysis, the Delft3D-FLOW module along with the FLOOD solution scheme is applied to simulate tsunami propagation and run-up at Units 6 & 7.

Delft3D-FLOW assumes hydrostatic pressure distribution, ignores frequency dispersion, and does not include wave breaking mechanism. As a result, model simulation results on tsunami propagation generally show steeper wave fronts with larger wave amplitudes compared to analytical solutions or benchmark laboratory test results (Reference 221). The shallow water conditions adopted in Delft3D-FLOW therefore are capable of resolving the tsunami wave propagation where the frequency dispersion is not significant and would be conservative in simulating the near shore tsunami amplitude.

2.4.6.4.2 Model Setup

AGMTHAG and Mader reported modeling of the 1755 Lisbon Earthquake tsunami and included most of the Atlantic Ocean in the model domain (References 202 and 209). The PMT model for Units 6

& 7, on the other hand, a portion of the Atlantic Ocean and the Gulf of Mexico are considered in the model setup, as described below.

Model Domain and Grids

To be able to investigate nearshore tsunami wave modification and onshore run-up, the tsunami model domain is selected to include detailed bathymetric variations in the area bounded by the Atlantic continental shelf, the Florida platform, Cuba, Dominican Republic, and the Blake-Bahama basin (as shown in Figure 2.4.6-209). In light of the uncertainties in defining the 1755 Lisbon Earthquake source in the Azores-Gibraltar region (References 202 and 209), tsunami generation at the source was not included in the model. Instead, the model (open) boundary in the Atlantic Ocean is established based on tsunami propagation patterns reported in existing literature, as described in Subsection 2.4.6.4.3.

The selected model domain is shown on Figure 2.4.6-210. The east model boundary in deep waters generally follows the simulated propagation of tsunami wave front after 6.5 hours of travel in Mader's analysis (Reference 209). The 6.5 hour wave front is selected to maximize the coverage of the ocean in the model and also allow the model to be defined by one open sea boundary with a uniform boundary condition. This open boundary extends from Havelock, North Carolina to north east of the Dominican Republic. The north and west model boundaries follow mostly the coastlines of the southeastern United States. The south model boundary is set along the northern coastlines of the Dominican Republic, Haiti, and Cuba. The small passage between Haiti and Cuba is conservatively assumed to be blocked. Southwest of the site, the model includes a portion of the Straits of Florida, the area protruding past the Florida Keys, to allow the tsunami wave to travel farther into the Gulf of Mexico so that the effect of this boundary on the site is minimized. Extending the model farther into the Gulf of Mexico is not necessary, as the maximum tsunami water level at the site would occur before the effect of this boundary is reflected back at the site. Consequently, the model boundary in the Gulf of Mexico is simulated as a closed boundary.

The model uses curvilinear orthogonal grids that are generated with RGFRID, the Delft3D module for grid generation and processing. The curvilinear option allows fitting grids cells along coastlines and contours of changing bathymetry. In addition, curvilinear grids could be oriented in relation to anticipated flow direction or wave propagation, thereby improving model accuracy.

A nested grid system with three different grid resolutions is developed using the domain decomposition tool within RGFRID to appropriately resolve tsunami wave modification near the site. The three grid subdomains are shown on Figure 2.4.6-210. The first

subdomain, SITE, covers the area near the site including the Biscayne Bay and the adjacent Straits of Florida, and has the finest grid resolution. The second subdomain, ISLANDS, includes most of the Bahamas with intermediate grid resolution. The third subdomain, DEEP, covers the rest of the model domain with a coarse grid resolution, which is mostly deep waters and is farther away from SITE and ISLANDS subdomains. At the interfaces between the subdomains, every third point in the finer grid is aligned with successive grid points in the coarser grid. Subdomain grid resolutions, represented by the square root of grid cell area, and grid spacings in the two orthogonal directions are given in Table 2.4.6-203. Figures 2.4.6-211 through 2.4.6-213 show the grids of the three subdomains.

Model Bathymetry

Tsunami model bathymetric and topographic data are obtained from the following public sources:

- Biscayne Bay sounding data from NOAA estuarine bathymetric database
- LiDAR (Light Detection And Ranging) data from NOAA Coastal Ocean Service database
- Coastal Relief data from NOAA National Geophysical Data Center (NGDC)
- ETOPO1 data from NOAA NGDC

The last two sources include both bathymetric and topographic (land) data, whereas the first source includes only bathymetric data, and the second source includes only topographic data. The four data sets have different horizontal and vertical resolutions. The Biscayne Bay sounding and LiDAR data have high vertical and horizontal resolutions compared to the Coastal Relief and ETOPO1 data. Therefore, they were given high priority and used first in populating the model depth data. The Coastal Relief data has higher horizontal resolution compared to the ETOPO1 data and therefore was given priority in populating the remaining model domain. A summary of resolution of available data is given in Table 2.4.6-204.

Bathymetric data from all sources are projected to the Azimuthal Equidistant map projection centered at Unit 6 & 7 for a uniform horizontal datum description. The Azimuthal Equidistant map projection is used to minimize distortion in both distance and direction from the site. All bathymetric and topographic elevations are converted relative to mean sea level (MSL) from their original source datum. Conversion relationships between MSL and various vertical datums are selected based on NOAA's Virginia Key, Florida station.

The bathymetric and topographic elevations for the tsunami model are developed by using the Delft3D-QUICKIN module. Elevations at the grid points are determined by interpolating from the source data surrounding the grid points. Model bathymetric elevations at grid points with seabed located below the MSL are specified as positive, whereas, all grid points on land are given negative bathymetric (topographic) values. The developed model bathymetric map is shown on Figure 2.4.6-214.

Bed Roughness Condition

Bed roughness conditions in the tsunami model are specified through Manning's n roughness coefficient. A constant Manning's roughness coefficient of 0.025 is used for the entire model domain, which represents natural channels in good condition (Reference 2.4.6-222).

Initial Condition

The antecedent water level including the 10 percent exceedance high spring tide, initial rise, and long-term sea level rise, as specified in Subsection 2.4.5.2.2.1, is used as the initial water level for the tsunami model. The initial water level in the tsunami model, after conversion to MSL, is 1.36 meters (4.46 feet) MSL.

Time Step and Simulation Time

The tsunami model is run with a time step of 0.2 minute (12 seconds). The model simulations are continued for a period of 9 hours, although the travel time from the open boundary to the site is about 2.5 hours and the maximum tsunami water level at the site is reached after about 4.5 hours from the start of simulation. Therefore, simulation period of 9 hours is sufficient to capture the maximum water level at the site. The start and end time for model simulations are selected arbitrarily.

2.4.6.4.3 Selection and Validation of Open Boundary Condition

2.4.6.5 Tsunami Water Levels

The model requires time history of incoming tsunami water level as the boundary condition along the eastern open boundary. However, no measured water level data from the 1755 Lisbon Earthquake tsunami is available at the model boundary location. Consequently, a synthetic time history of tsunami water level assuming a sinusoidal tsunami waveform is used to establish the model boundary condition.

Tsunami water level on the Atlantic coast near Miami, Florida, is obtained from the model simulation results performed by Mader for the 1755 Lisbon Earthquake tsunami (Reference 209). Because the source location and characteristics for the 1755 Lisbon Earthquake are not precisely known, Mader developed tsunami source parameters in such a way that the

model reproduces tsunami amplitude and arrival time within reasonable accuracy at near- and far-field locations where these are known. Mader assumed the source location to be close to Gorringer Bank in the Azores-Gibraltar region, near the source location of the 1969 earthquake (1969 earthquake location is shown on Figure 2.4.6-206). To produce a tsunami amplitude of 20 meters (65.6 feet) with a 1-hour wave period that arrives at Lisbon, Portugal, 40 minutes after the earthquake, Mader considered fracture in a 300 kilometers (186.4 miles) arc-fault with a slip of 30 meters (98.4 feet). Although Mader did not provide information on the strike angle or location, the curved fault structure resembles closely to the composite fault zone assumed by Gutscher et al. in 2002, 2006 and discussed in AGMTHAG (Reference 202). In addition, the slip magnitude assumed by Mader is higher than that listed in Subsection 2.4.6.3.

AGMTHAG also performed numerical model simulations of the 1755 Lisbon Earthquake tsunami to evaluate the potential tsunami impact on the U.S. east coast. AGMTHAG first investigated the constraints on the earthquake epicenter from far field simulations. AGMTHAG modeled three different source segments for the northern Puerto Rico/Lesser Antilles subduction zone including the Hispaniola, Puerto Rico, and Virgin Island faults. The earthquake moment magnitude from the selected source parameters ranges between 9.11 and 9.15. Using a linear long-wave model, AGMTHAG obtained a maximum tsunami amplitude near the site to be no more from than 0.1 meter (0.3 foot), as described in Subsection 2.4.6.1.5. AGMTHAG simulated tsunami propagation for 16 such potential source locations as shown in Figure 2.4.6-209²¹⁵. Based on model simulation results, AGMTHAG concluded that the variation in local seafloor bathymetry significantly controls tsunami propagation across the Atlantic Ocean. The Gorringer Bank and the Madeira Trench Rise (see Figure 2.4.6-206 for locations) act as near source barriers protecting most of the U.S. east coast. For sources located east of Madeira Trench Rise and south of Gorringer Bank, Florida might be at risk if sufficient wave energy passes through the Bahamas (Reference 202). AGMTHAG did not simulate tsunami wave run-up in the near shore region and considered relative amplitude evaluation only (Reference 202). Because the simulated deepwater tsunami amplitude in the southeastern U.S. coast from AGMTHAG is smaller than the tsunami amplitude reported in Mader (References 202 and 209), the present analysis adopted tsunami amplitude from Mader as the amplitude for the PMT **in developing the boundary condition for the tsunami model.**

Mader performed numerical modeling of the tsunami wave using the SWAN nonlinear shallow water wave code including the effects of Coriolis and friction effects. The model domain extended from 20° N to 65° N and 100° W to 0° W with a 10-minute grid resolution. Model bathymetry information was generated from the 2-minute Mercator Global Marine Gravity topography of Sandwell and Smith of the Scripps Institute of Oceanography (Reference 209). A model time step of 10 seconds was used for the simulation. Mader obtained tsunami amplitude of 20 meters

(65.6 feet) at 953 meters (3127 feet) water depth off Lisbon, Portugal, and 5 meters (16.4 feet) at 825 meters (2707 feet) water depth east of Saba, Netherlands Antilles in the Caribbean. Mader argued that with a run-up amplification of the wave, the maximum near-shore wave amplitude would be two to three times the deepwater tsunami amplitude. However, he also pointed out that some of the run-up effects were probably included in the simulation for water depths less than 1000 meters (3281 feet). This assumption would provide a maximum tsunami water level above 20 meters (65.6 feet) at Lisbon and above 7 meters (23 feet) at Saba, higher than the tsunami amplitudes reported by Lockridge et al. (Reference 208). Consequently, simulated water levels obtained by Mader along the U.S. east coast would likely be conservative. Mader obtained tsunami amplitude of 2 meters (6.6 feet) at 783 meters (2569 feet) water depth east of Miami, Florida **with a tsunami period of 1.5 hours**, and suggested a maximum tsunami wave amplitude, including run-up, of approximately 10 feet (3 meters) along the U.S. east coast (**Reference 209**).

~~Several tsunami simulations are reported for the earthquakes in the northern Caribbean region, as presented in Subsection 2.4.6.1.2 (References 202 and 211). The maximum tsunami amplitude near the southern Florida Atlantic coast (near Virginia Key) from these studies is approximately 0.15 meter (0.5 foot), as obtained by Knight (Reference 211). AGMTHAG used a linear shallow water model for the simulation with source parameters slightly different from those listed in Subsection 2.4.6.3.2. Knight assumed an earthquake magnitude of $M_w = 9.0$ in the Puerto Rico trench (Reference 211), higher than the earthquake magnitude presented in Subsection 2.4.6.3.2. These simulations show higher tsunami amplitude along the U.S. Mid-Atlantic region, as described in Subsections 2.4.6.1 and 2.4.6.2. However, simulated tsunami amplitude along the U.S. southeast coast as a result of the earthquake in the Azores-Gibraltar fracture zone (by Mader) is higher than the tsunami amplitude from the Caribbean sources (by Knight).~~

~~As suggested by Mader, the maximum deepwater tsunami amplitude near Miami, Florida, would be approximately 2 meters (6.6 feet) with a period of approximately 1.5 hours (Reference 209). Assuming that the onshore maximum tsunami amplitude including run-up would be approximately twice the deepwater value, a maximum tsunami amplitude of 4 meters (13.1 feet) can be obtained corresponding to the PMT. This value is a conservative estimate because the presence of the Bahamas platform is expected to considerably reduce the tsunami amplitude before reaching Units 6 & 7. In addition, Mader suggested that the maximum tsunami amplitude along the U.S. east coast to be approximately 3 meters (10 feet) (Reference 209).~~

The synthetic tsunami marigram at the model boundary is selected such that the maximum tsunami wave amplitude and drawdown off Miami, Florida at a water depth of 783 meters (2569 feet) are comparable or conservative compared to Mader's results for the same location. Mader estimated the maximum wave amplitude and

drawdown of 2.0 meters (6.6 feet) and -3.5 meters (-11.5 feet), respectively, from the initial water level at MSL (Reference 209). To generate the tsunami marigram at the model boundary, three different sinusoidal wave patterns are considered, each with 2.0 meter (6.6 feet) amplitude and 1.5 hours wave period. The first case considers a single wave, the second case considers a continuous wave train, and the third case considers only two consecutive waves. Figure 2.4.6-216 shows the marigrams for the three cases.

Figure 2.4.6-217 shows the simulated tsunami water levels for the three selected cases at the 783 meters (2569 feet) water depth off Miami, Florida. Similar to Mader, model simulations for the three cases consider the initial water level to be at MSL. Continuous wave train at the boundary generates the maximum tsunami amplitude and drawdown of about 5.5 meters (18 feet) and -6.5 meters (-21.3 feet), respectively, with respect to the MSL. These amplitude and drawdown are much higher than what is indicated in Mader's analysis, and therefore model input conditions with continuous wave train are not considered to be realistic. The single wave boundary condition produced the maximum wave amplitude and drawdown of about 2 meters (6.6 feet) and -3.5 meters (-11.5 feet), respectively, which are in very good agreement with Mader's results. However, because more than one wave was reported to have impacted the Portuguese and Canadian coasts (References 208 and 209), the single wave boundary condition is not considered in the present analysis. The boundary condition with two consecutive waves generates the maximum wave amplitude and drawdown of 4.5 meters (14.8 feet) and -5.3 meters (-17.4 feet), respectively. Although these values are much higher compared to Mader's results, they are conservatively adopted for this analysis. This tsunami amplitude is also much higher than the tsunami amplitudes reported in AGMTHAG for many different earthquake source locations and orientations in the Azores-Gibraltar fracture zone and for the Caribbean sources (Reference 202).

2.4.6.4.4 Sensitivity of Model Parameters

Model sensitivity analysis is conducted for the following parameters: grid size, time step, Manning's n value, tsunami wave period, and Coriolis effects.

Grid Size

Model grid configuration is selected based on bathymetric data resolution, computational economy, etc. A finer mesh model grid is developed as part of grid size sensitivity analysis to demonstrate that the selected grid sizes resolves the required flow problems reasonably well. In the finer mesh model, grid sizes for the ISLANDS and SITE subdomains are refined by a factor of 5/3 (1.67), whereas the grid sizes in subdomain DEEP remained unchanged because of

computational economy. Additionally, because the DEEP subdomain is located farther away from the site and in high water depths, a finer grid resolution in this area is not expected to produce any significant variation in tsunami water level at the site. The difference in tsunami water levels at the site from the two grid descriptions is very small, as shown in Figure 2.4.6-218. The selected coarser grid configuration therefore is considered adequate.

Time Step

Model simulations are performed with a computational time step of 0.2 minute (12 seconds). However, to demonstrate time step independence, a model simulation with 0.1 minute (6 seconds) time step is performed. Because the water levels at the site from the two simulations are nearly identical, the use of 12 seconds time step is considered acceptable.

Manning's n value

Model simulations are performed for two additional Manning's n values of 0.02 and 0.03. The results indicate that a lower Manning's n value produces a higher water level at the site. However, for this analysis a Manning's n of 0.025 is selected based on typical coastal area surface characteristics (Reference 222). Because the selected boundary condition provides conservative tsunami amplitude at the site, as described in Subsection 2.4.6.4.3, the selected bed roughness conditions are considered adequate.

Tsunami Wave Period

Mader indicated that for the 1755 Lisbon Earthquake tsunami, the eastern U.S. coast, and the Caribbean would experience tsunami wave periods varying between 1.25 and 1.5 hours (Reference 209). Results from an additional model simulation with a tsunami wave period of 1.25 hours show that the maximum water level at the site is lower than maximum water level from the selected wave period of 1.5 hours. Therefore, the selected wave period is adopted in this analysis.

Coriolis Effects

Coriolis forces depend on the latitude and angular velocity of earth's rotation on its own axis. Model simulation results with and without Coriolis forces indicate that the effect of Coriolis force on the maximum water level at the site is insignificant. Coriolis forces therefore are not considered in model simulations.

~~Consistent with RG 1.59, a 10 percent exceedance high spring tide and sea level anomaly (initial rise) is used as the antecedent water level for the storm surge during a probable maximum hurricane event. The same antecedent water level condition is also used to obtain the PMT maximum water level. As described in Subsection 2.4.5, the combined 10 percent exceedance high spring tide and initial rise as given in RG 1.59 for the Miami Harbor Entrance is higher than the~~

maximum historical tidal levels recorded at the National Oceanic and Atmospheric Administration tide gages near Units 6 & 7. Therefore, the combined 10-percent exceedance high spring tide and initial rise of approximately 2.6 feet NAVD 88, which is equivalent to 4.5 feet above mean low water as given in RG 1.59 and Subsection 2.4.5, is conservatively assumed for Units 6 & 7. Additionally, the probable maximum hurricane event considers a nominal long-term sea level rise of 1.0 foot for the next 100 years, as described in Subsection 2.4.5. Combining the 10-percent exceedance high tide and initial rise (2.6 feet NAVD 88) and the longterm sea level rise (1.0 foot) with the postulated conservative PMT amplitude near Units 6 & 7 (13.1 feet or 4 meters), the PMT maximum water level at Units 6 & 7 is 16.7 feet NAVD 88. The maximum water level estimated at Units 6 & 7 as a result of the PMT is below the maximum storm surge level, as presented in Subsection 2.4.5.

The PMT event could also induce a water surface drawdown at the Florida Atlantic coast shoreline. Off the coast of Miami, Florida, a minimum tsunami drawdown (trough) of approximately 3.5 meters (11.5 feet) at a water depth of 783 meters (2569 feet) is reported from the model simulation of Mader with a period of approximately 1.5 hours (Reference 209). A similar low water level may be considered for the Atlantic coast near Units 6 & 7. Because of the presence of the chain of barrier islands offshore of Biscayne Bay including Elliott Key, the drawdown water level at the shoreline would have a reduced effect on the low water level within the Biscayne Bay. Furthermore, because the Units 6 & 7 do not rely on Biscayne Bay for plant safety related water supply, low water levels in the bay as a result of tsunami drawdown would not affect the functions of the safetyrelated SSCs at Units 6 & 7.

2.4.6.4.5 Model Simulation Results

As described in Subsections 2.4.6.4.2 and 2.4.6.4.3, the maximum tsunami water level at the site is simulated for a boundary condition with two consecutive sinusoidal tsunami waves of 2.0 meters (6.6 feet) amplitude and 1.5 hours wave period. This boundary condition approximates the 1755 Lisbon tsunami that was generated at the Azores-Gilbaltar region, as simulated by Mader (Reference 209). An initial water surface elevation of 1.36 meters (4.46 feet) MSL is used to evaluate the maximum tsunami water level at the site.

Water level contours at different times are plotted to track the tsunami wave propagation from the open boundary to the site. These time-lapsed snap-shots of water level contours are given in Figures 2.4.6-219a through 2.4.6-219i. As the figures indicate, the tsunami waves propagate from the open boundary to Blake-Bahama Escarpment unimpeded and nearly perpendicular to the escarpment. As the waves reach the Bahama platform, tsunami waves north of the platform (north of Grand Bahama and Abaco Islands) are diffracted southwestward towards the Straits of Florida. The diffracted waves propagate through the Straits of Florida before reaching the site. The tsunami waves reaching the platform are affected by shoaling and travel through the channels and passages

between the islands of the Bahamas. These transmitted tsunami waves then interact with the diffracted waves from the north.

From the Straits of Florida the tsunami waves enter the Biscayne Bay first through the openings, cuts, and channels in the barrier islands, and then by overtopping the barrier islands before affecting the site. The maximum tsunami water level at the site is reached as the barrier islands are overtopped. Water level contours in Biscayne Bay corresponding to the time close to the maximum water level at the site is shown in Figure 2.4.6-220.

The site is protected by the Bahamas from direct impact of the tsunami waves. The diffracted tsunami waves have less energy and therefore less flooding potential at the site. In addition, the islands and the vast extent of the Bahamas dissipate some of the tsunami wave energy before it reaches the deep waters of the Straits of Florida and ultimately the site.

Time history of tsunami water levels at key locations are plotted to show tsunami wave modification as it propagates and reaches shore. Figures 2.4.6-221a through 2.4.6-221d show the locations of the water level monitoring points. Track 1 (Figure 2.4.6-221a) generally follows tsunami wave propagation from the open boundary to east of the Bahamas and then the diffraction towards the Straits of Florida. The tsunami marigrams for the monitoring points are given in Figure 2.4.6-222. The figure shows that as the tsunami waves travel from the open boundary towards the Bahamas, its amplitude increases due to shoaling. The maximum shoaling is seen near the edge of the escarpment north of Little Bahama Bank at monitoring point 4. Waves then dissipate on the shallow waters and diffract towards the Straits of Florida (points 5 and 6). The tsunami amplitudes increase as the diffracted waves interact with the waves passing through the Islands of the Bahamas (points 6 and 7). However, as the tsunami waves travel further south towards the site, its amplitude decreases slightly due to propagation and possibly friction loss.

For Track 2 (Figures 2.4.6-221b and 2.4.6-223), tsunami amplitudes increase as the waves shoal east of the Bahamas similar to that observed for Track 1. Between monitoring points 3 and 4, tsunami amplitude decreases slightly. At monitoring point 5 south of Grand Bahama Island, where the depth is relatively shallow, the wave amplitude increases due to shoaling. In the Straits of Florida, wave modifications are the same as described for Track 1.

Track 3 (Figures 2.4.6-221c and 2.4.6-224) shows modifications of tsunami wave amplitudes along the eastern U.S. Atlantic coast. Between monitoring points 1, 2, and 3, tsunami amplitudes remain nearly the same while the arrival time changes due to their distance from the boundary. However, tsunami amplitudes at monitoring

points 4 through 7 are higher owing to the interaction of diffracted and propagated waves from the Bahamas.

Figure 2.4.6-225 shows tsunami marigrams in Biscayne Bay and vicinity. Grid cells (339, 270) and (339,232) are located within the Straits of Florida adjacent to the site; grid cell (339,172) is located between Biscayne Bay and the Straits at a shallow water depth (6.1 meters); and grid cells (339, 132), (339, 119), (307, 125), and (272, 146) are located within Biscayne Bay (Figure 2.4.6-221d). As shown in the figure, tsunami amplitudes within the Straits at the selected locations including the location with shallow water depth remain nearly the same. Water level variations within the Biscayne Bay, however, are markedly different compared to that in the Straits of Florida with the minimum water level in the bay considerably higher. This is because the barrier islands do not allow quick draining of the bay during tsunami drawdowns. In addition, the barrier islands dissipate wave energy during overtopping resulting in smaller wave amplitude and delayed arrival.

2.4.6.5 Tsunami Water Level

The time history of tsunami water level at the site is given in Figure 2.4.6-226. The maximum tsunami water level at the site from model simulation results is 4.17 meters (13.7 feet) MSL or 12.8 feet (3.9 meters) NAVD 88 including the initial water level of 1.36 meters (4.46 feet) MSL, which is rounded up to 14.0 feet (4.3 meters) NAVD 88. This maximum tsunami water level is 12 feet lower than the entrance floor elevation of all safety-related structures at 26 feet NAVD 88.

The following references will be added to Subsection 2.4.6.8 in a future revision.

217. ODP Shipboard Scientific Party, "Chapter 5. Site 626: Straits of Florida," *Proceedings Ocean Drilling Program*, Initial Report 101, p. 49-109, Austin, J. A. Jr., and Schlager, W. P., eds., 1986.
218. Iturralde-Vinent, M.A. (Ed.), *Geologia de Cuba para Todos, Edicion Cientifica, Museo Nacional de Historia Natural-CITMA*, preprint, 114 pages, 2009.
219. Deltares, *Delft3D-FLOW, Simulation of Multi-Dimensional Hydrodynamic Flows and Transport Phenomena, Including Sediments*, Rotterdamseweg 185, 2009.
220. Stelling, G.S., and Duinmeijer, S.P.A., "A Staggered Conservative Scheme for every Froude Number in Rapidly Varied Shallow Water Flows", *International Journal for Numerical Methods in Fluids*, volume 43, pp. 1329-1354, 2003.
221. Apotsos, A., Buckley, M., and Gelfenbaum, G., "Tsunami Benchmark Simulations Using Delft3D," *ISEC Community Workshop: Simulation & Large-Scale Testing of Nearshore Wave Dynamics, July 8-10, 2009 - Corvallis, Oregon*, 2009.

222. Imamura, F., Yalciner, A. C., and Ozyurt, G., *Tsunami Modeling Manual*, International Oceanographic Commission, 2006.

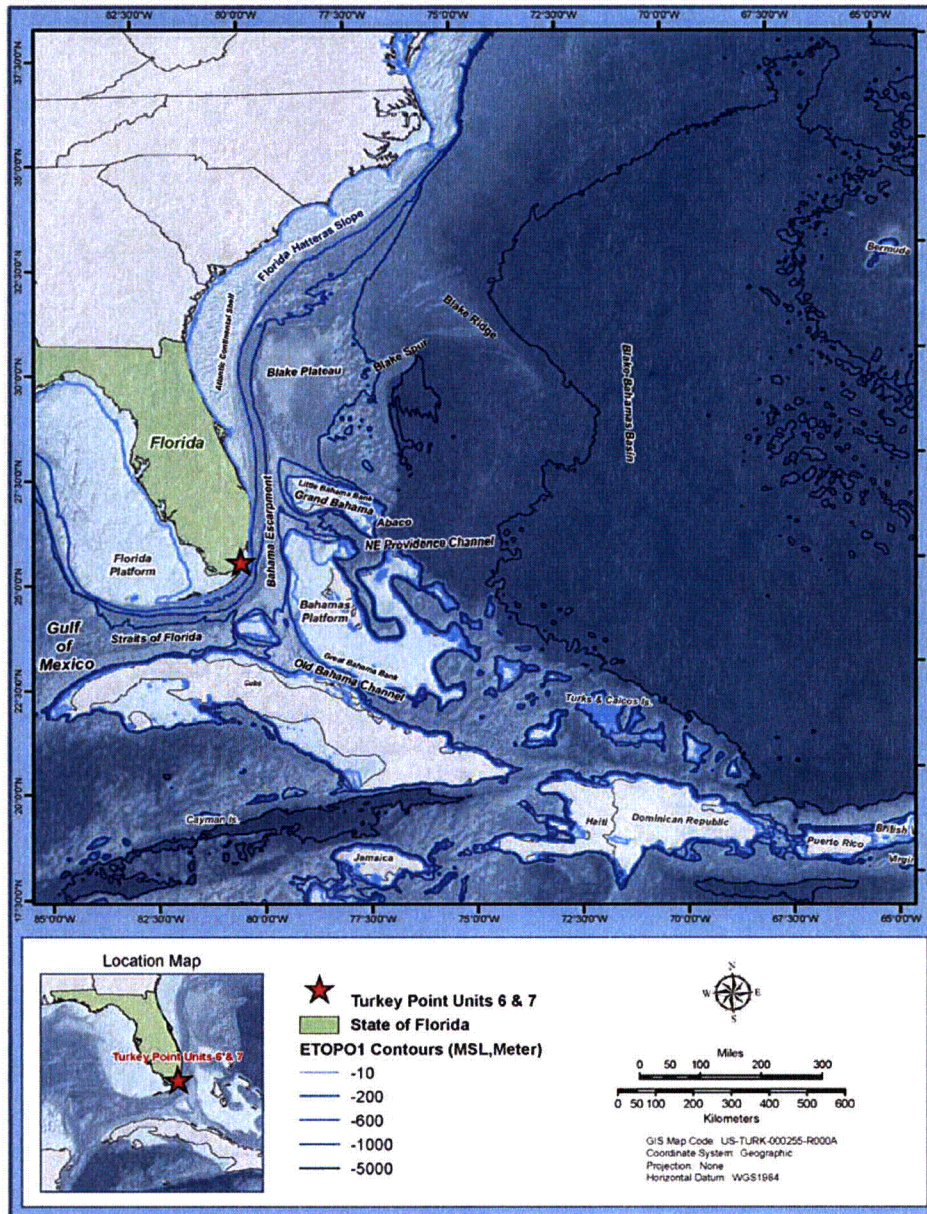
The following tables will be added to FSAR Section 2.4.6 in a future revision.

Table 2.4.6-203 Grid Resolution and Sizes of the Subdomains			
	Grid Resolution (m)	Grid Spacing along M^(a) Axis (m)	Grid Spacing along N^(a) Axis (m)
SITE	450 - 540	260 – 410	620 – 800
ISLANDS	1,240 – 3,710	970 – 3,010	950 – 7,050
DEEP	3,120 – 22,320	1,850 – 24,080	2,630 – 27,340
(a) M and N are the principal axes of the model curvilinear grid system			

Table 2.4.6-204 Horizontal and Vertical Resolutions of Depth Data				
	Biscayne Bay Sounding	LiDAR	Coastal Relief	ETOPO1
Horizontal Resolution	30 m	0.1 m^(a)	3 arc-seconds (90 m)	1 arc-minute (1,800 m)
Vertical Resolution	0.01 m	0.01 m	1 m for land 0.1 m for sea	1 m
(a) ~ 1 meter resolution for about 10 percent of the data				

The following figures will be added to FSAR Section 2.4.6 in a future revision.

Figure 2.4.6-209 Geophysical Setting and Seafloor Topography East of Southeast U.S. Coast and North of the Caribbean



**Figure 2.4.6-210 Extent of Selected Tsunami Model Domain and Subdomains
SITE, ISLANDS, and DEEP**

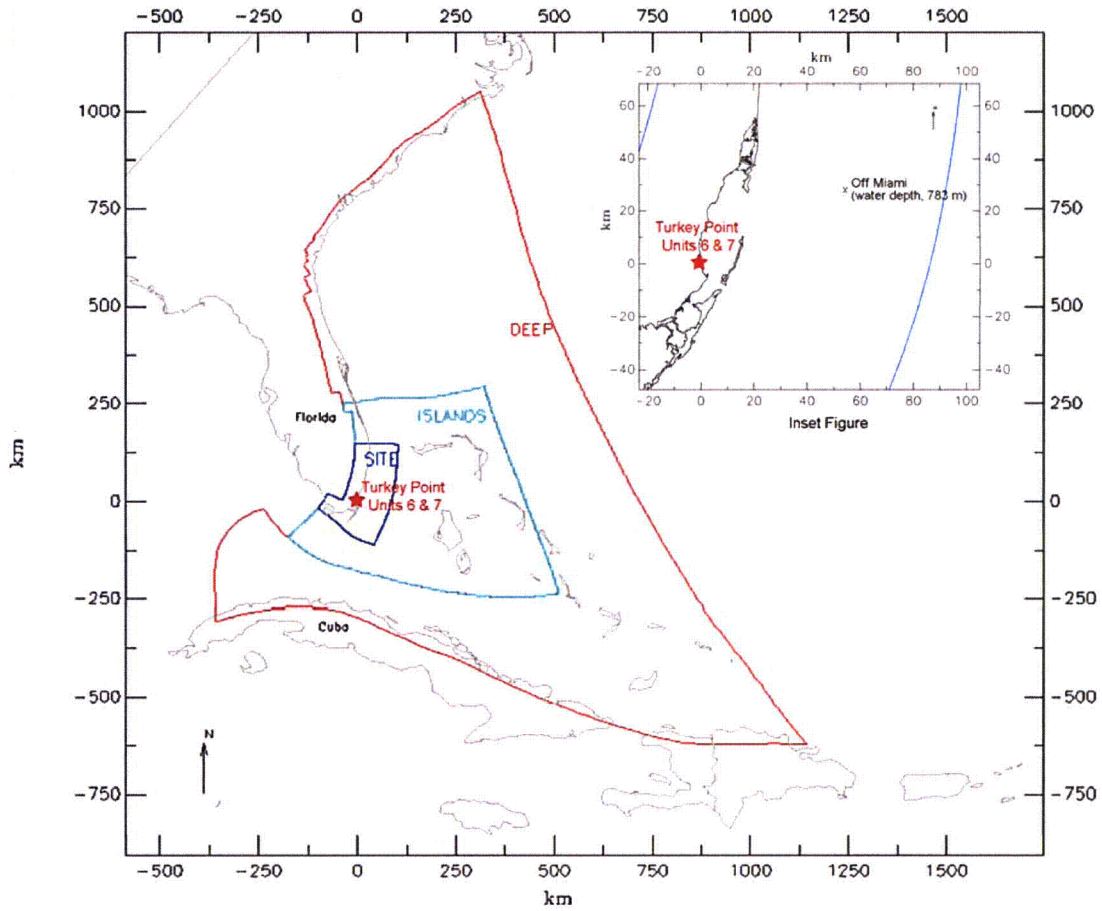


Figure 2.4.6-211 Model Grids of the DEEP Subdomain

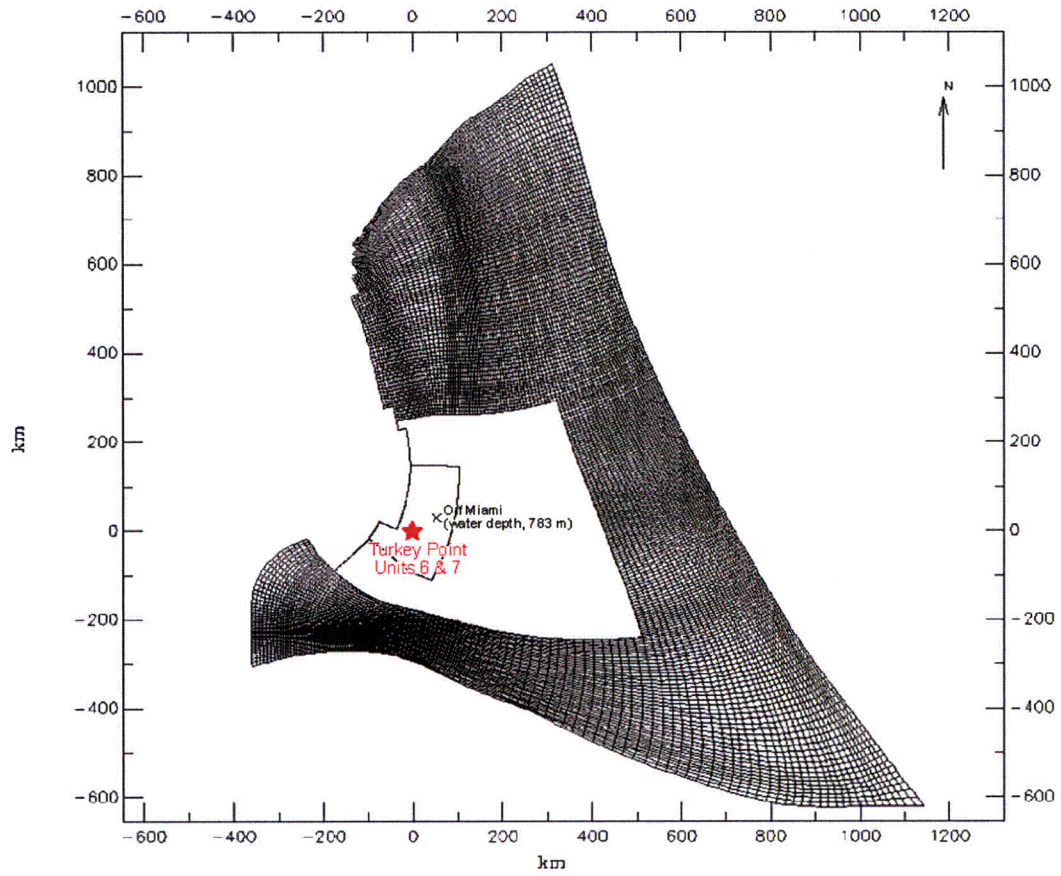


Figure 2.4.6-212 Model Grids of the ISLANDS Subdomain

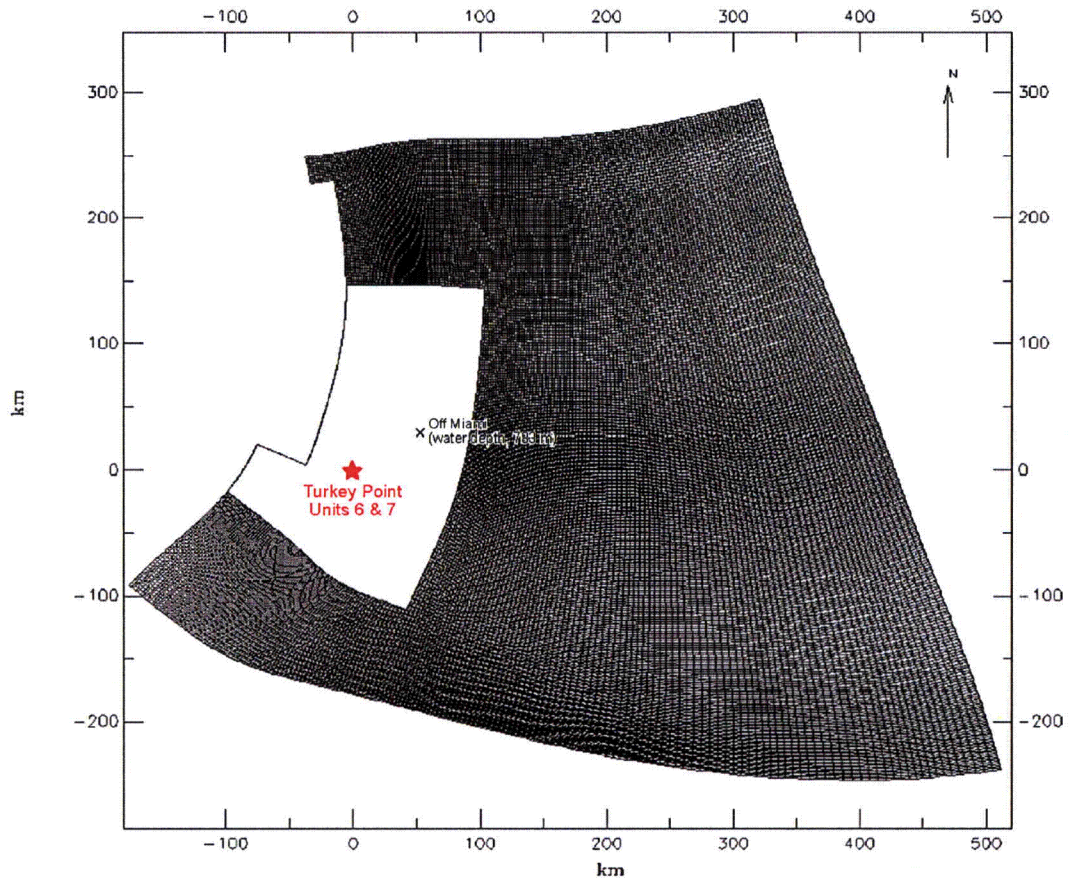


Figure 2.4.6-213 Model Grids of the SITE Subdomain near Units 6 & 7

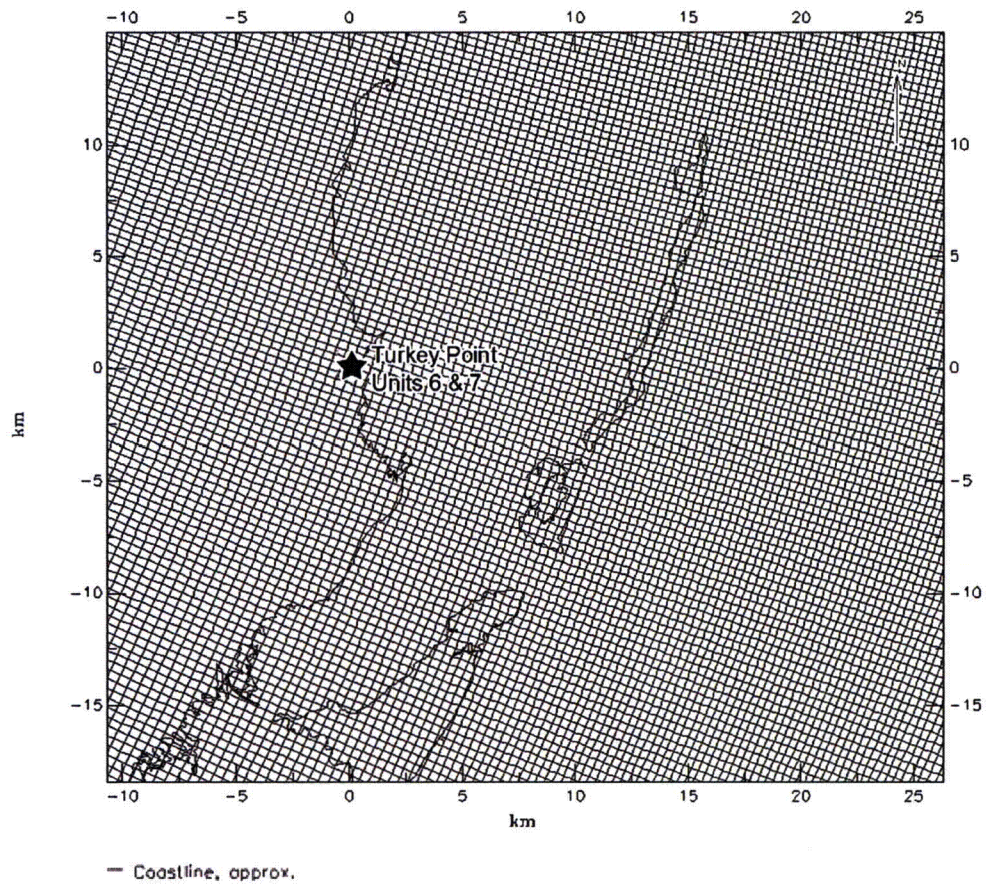
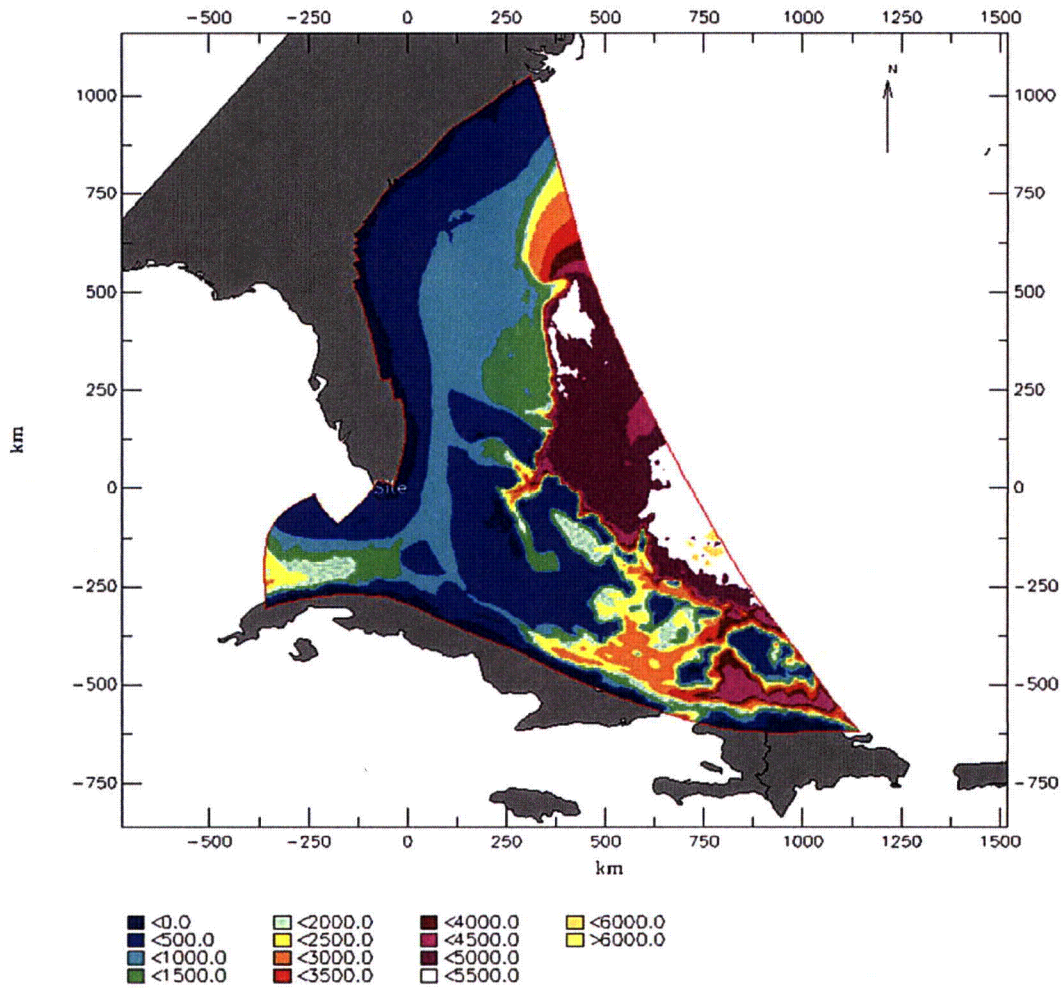
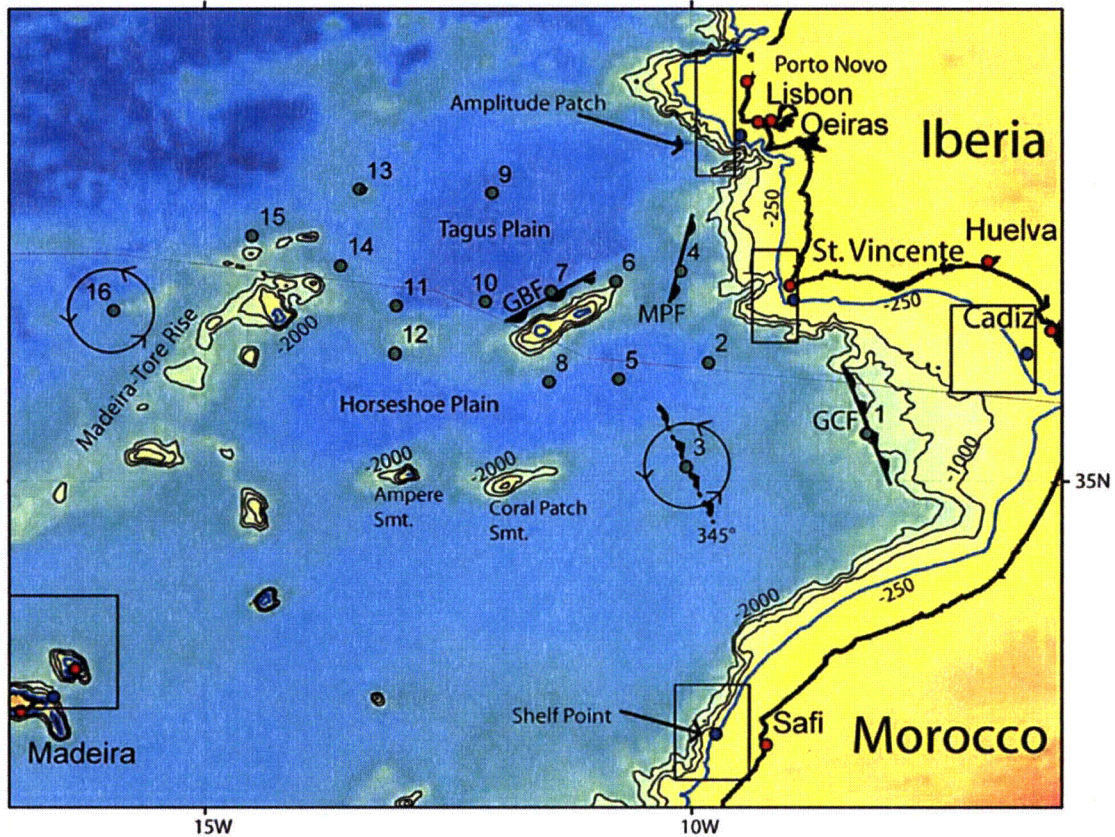


Figure 2.4.6-214 Contours of Model Bathymetry



Note: Depths to the seabed are in meters relative to MSL

Figure 2.4.6-209 **215** Postulated Epicenter Locations for the 1755 Lisbon Earthquake by
AGMTHJAGA **AGMTHAG**



Note: Fault orientation for source locations 3 and 16 were rotated 360° at 15° to test the optimal strike angle generating maximum tsunami amplitude in the Caribbean. Depth contours are in meters.
Source: Reference 202

Figure 2.4.6-216 Input Tsunami Marigrams at the Model Open Boundary for Conditions with Single Wave, Continuous Wave Train, and Two Consecutive Waves

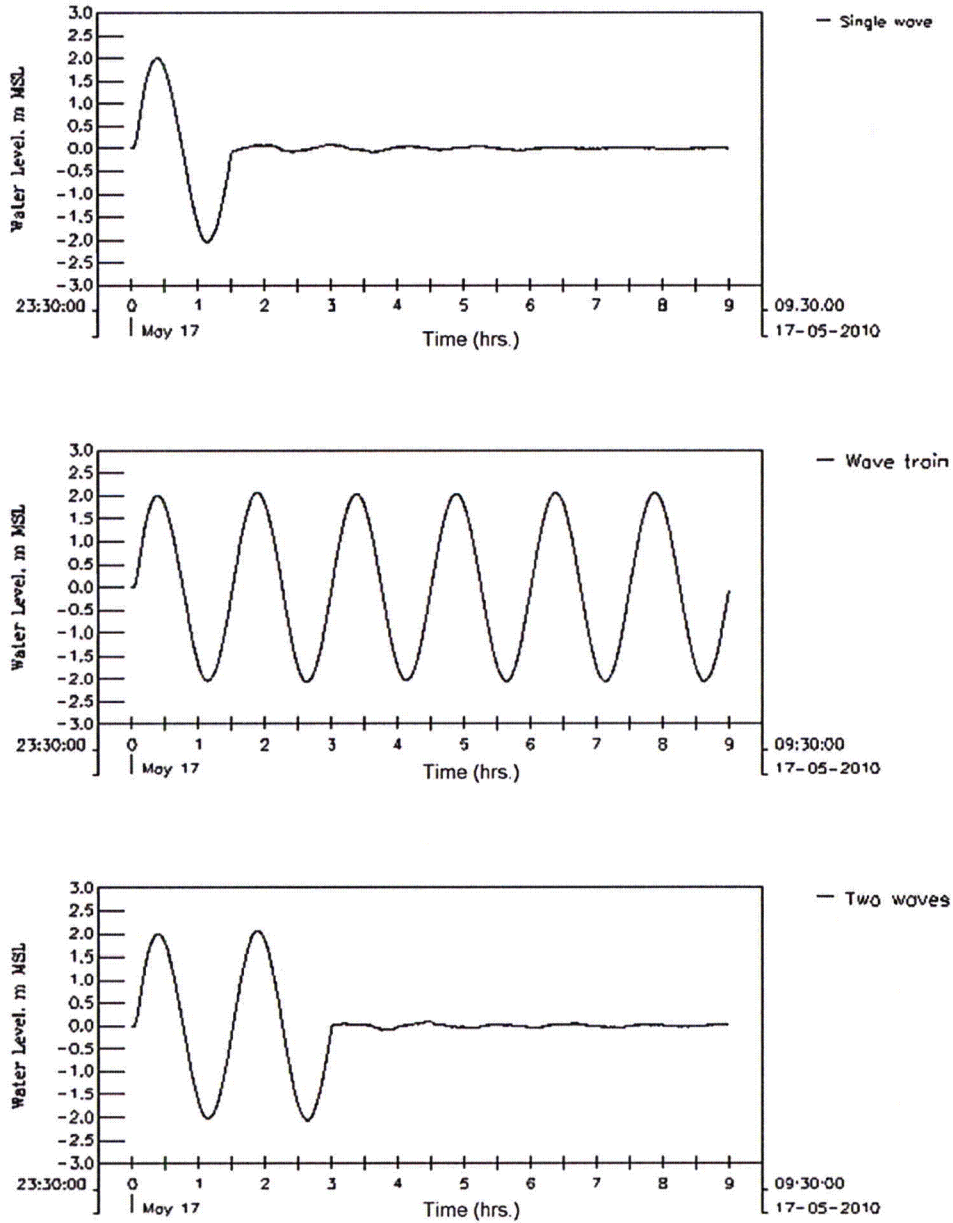
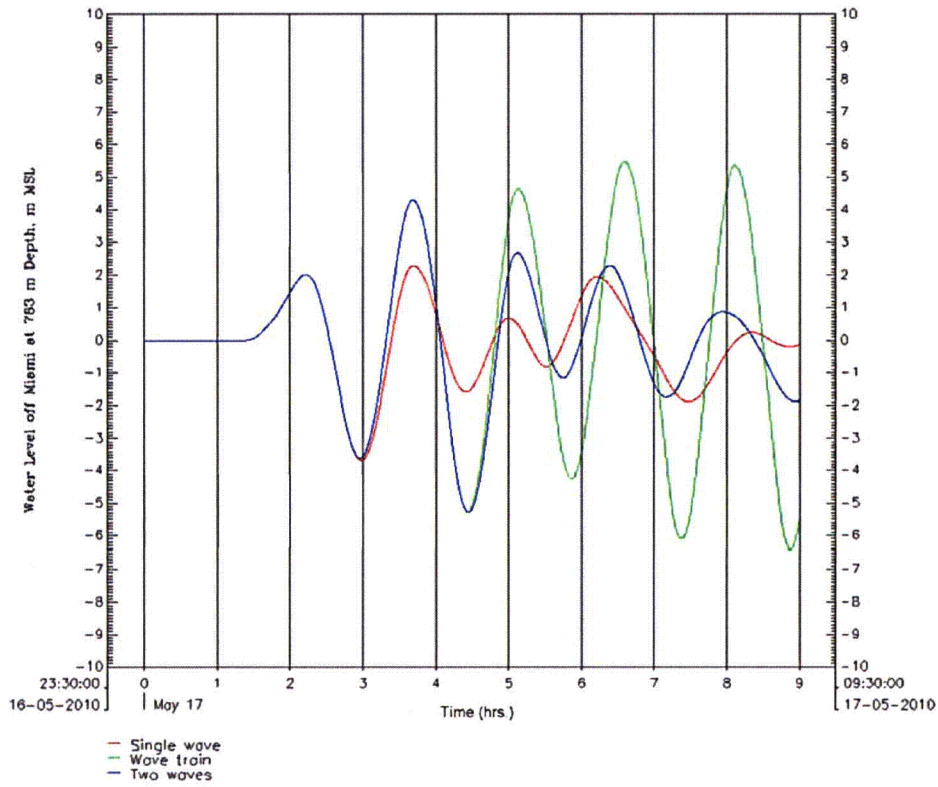
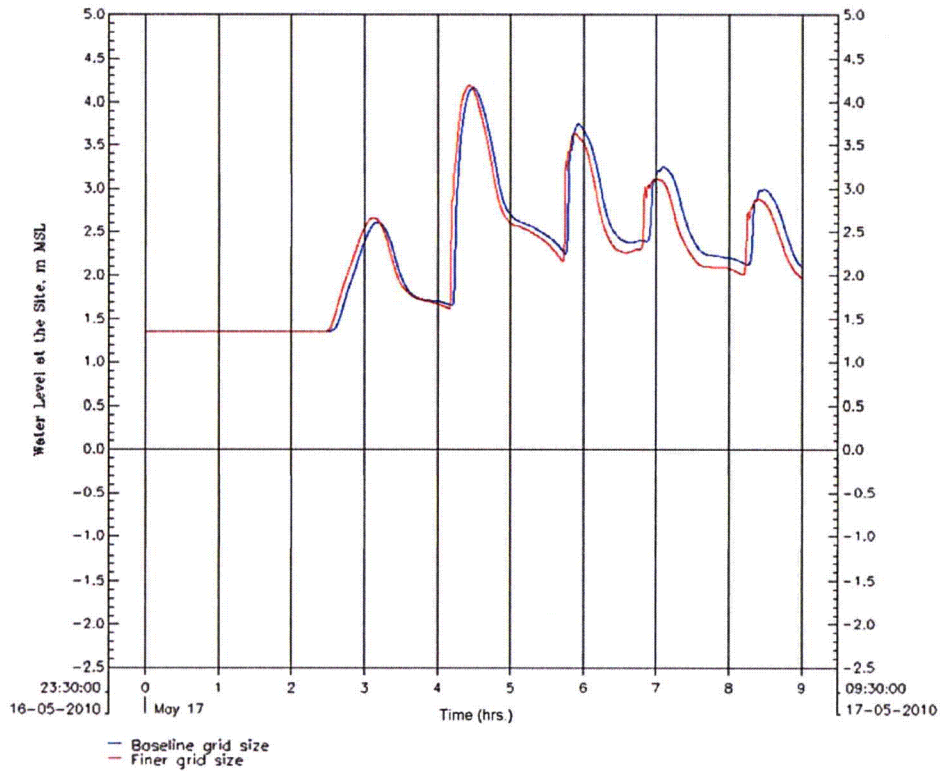


Figure 2.4.6-217 Simulated Tsunami Marigrams at 783 meters (2569 feet) Water Depth off Miami, Florida



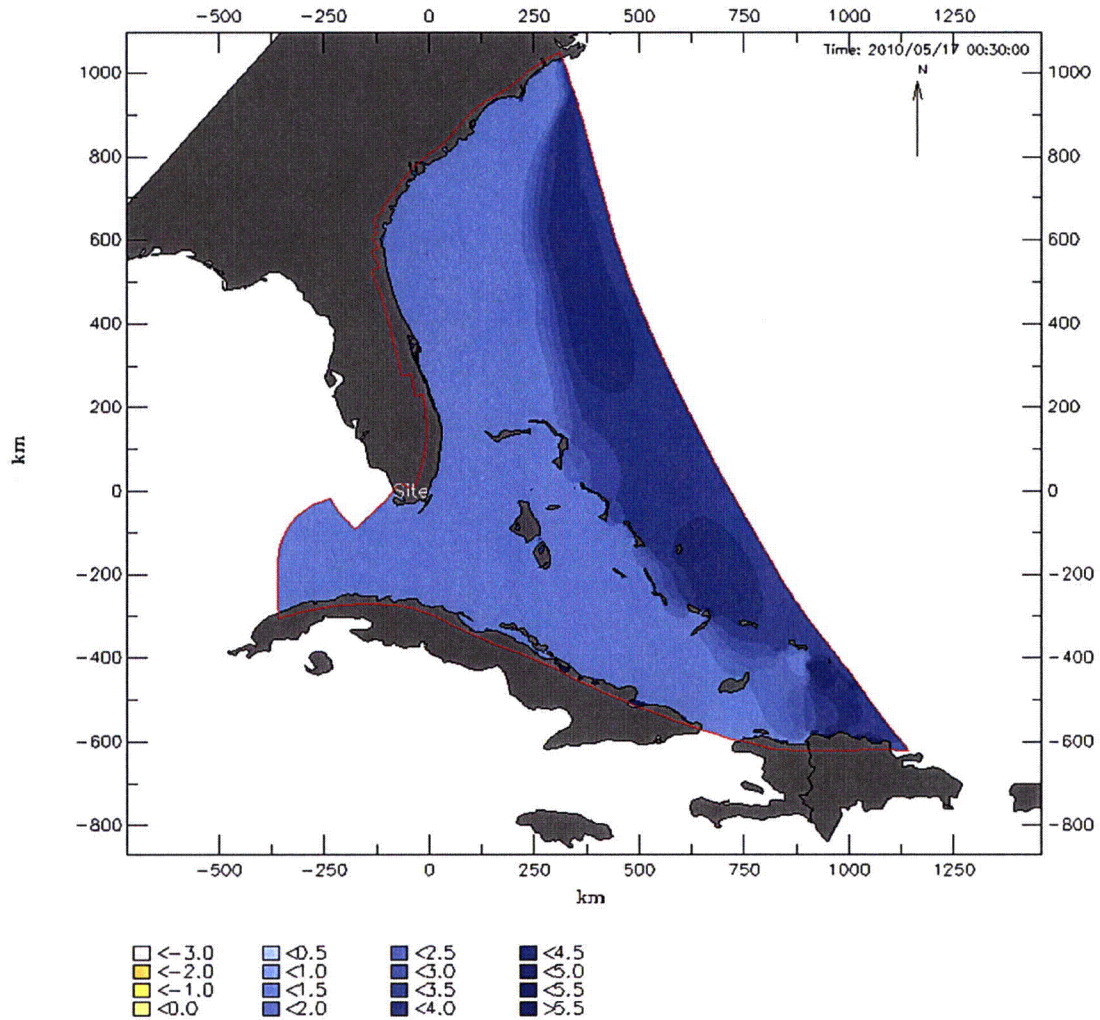
Note: Initial water level at MSL.

Figure 2.4.6-218 Simulated Tsunami Water Levels at the Units 6 & 7 Site for the Selected (Baseline) and Finer Grid Sizes



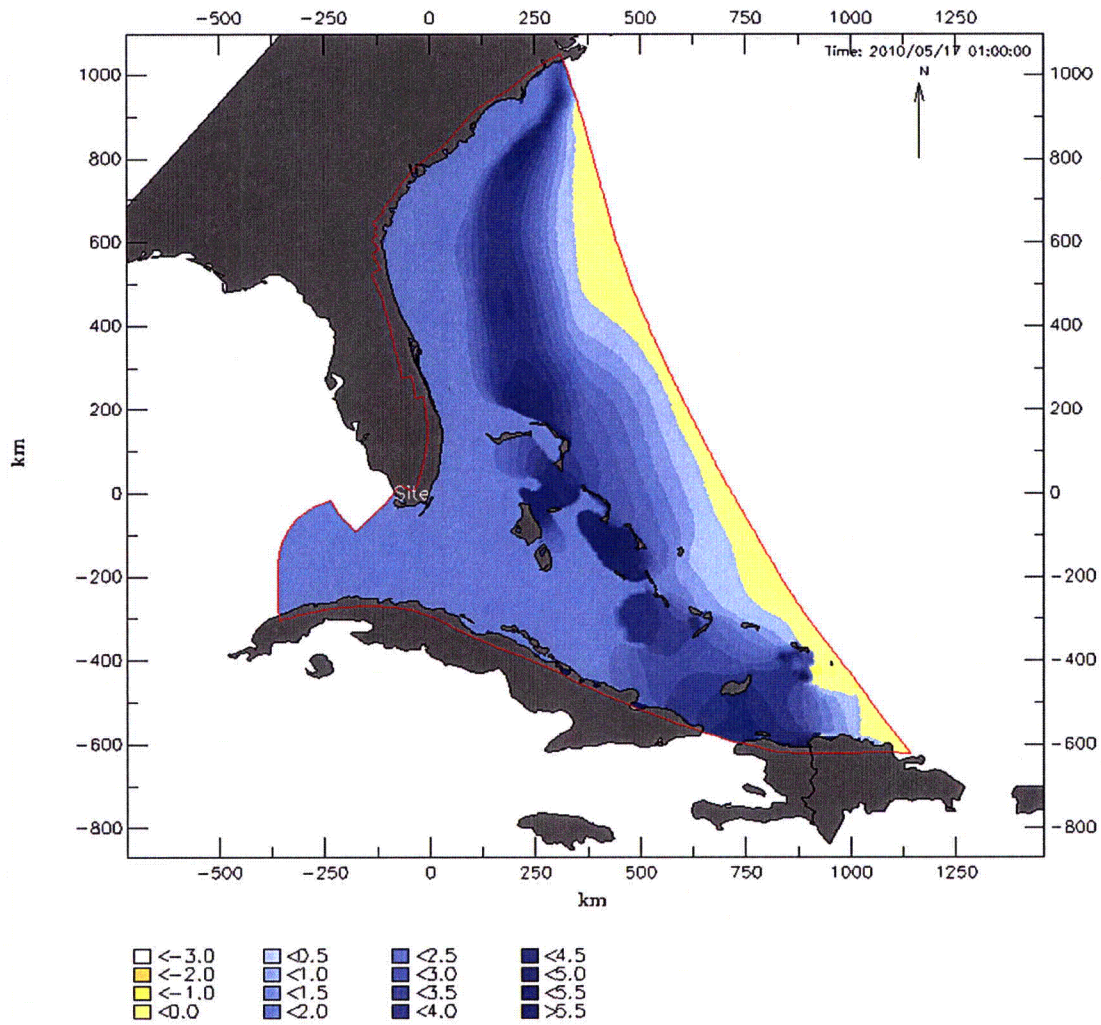
Note: Initial water level at 1.36 meters (4.46 feet) MSL.

Figure 2.4.6-219a Tsunami Water Level Contours 30 Minutes into the Model Simulation



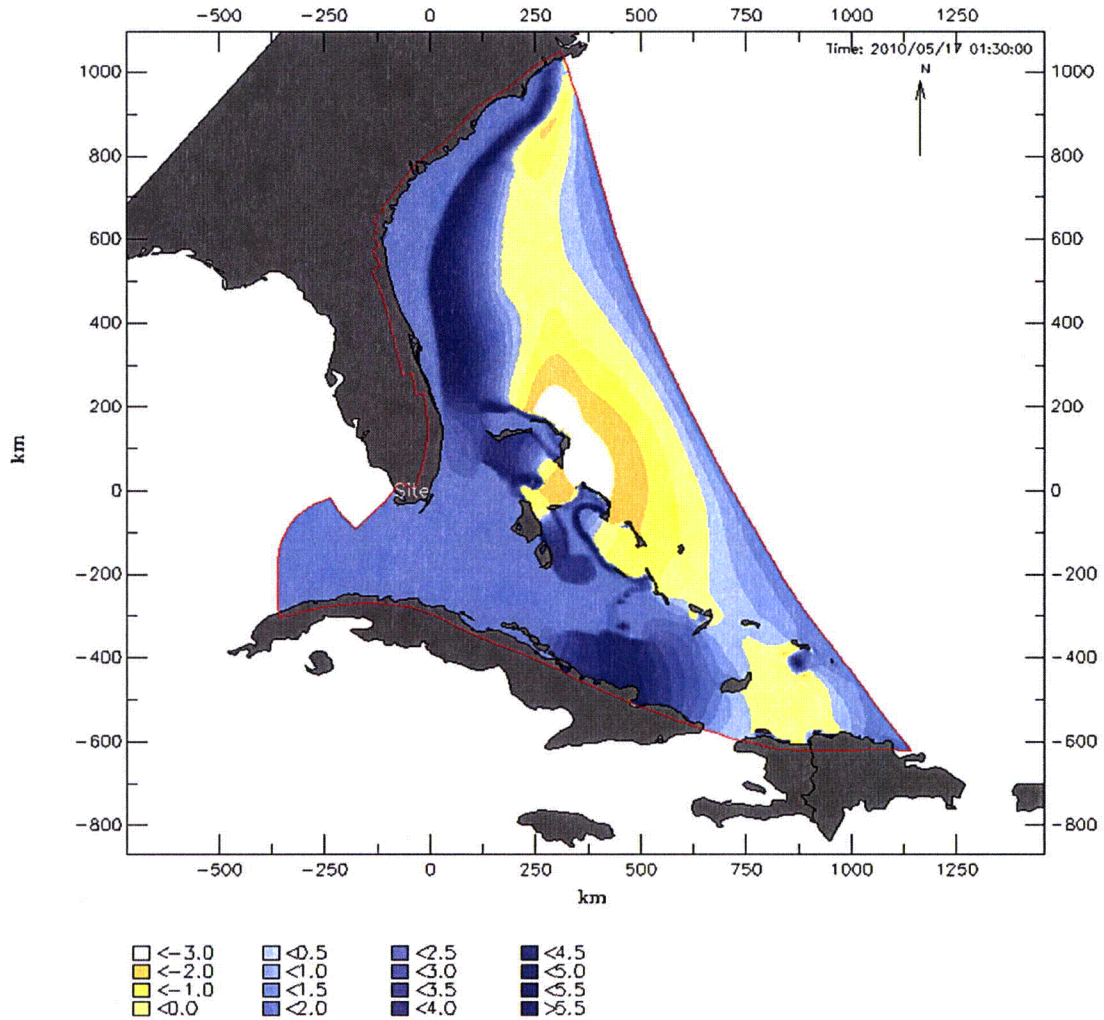
Note: Water levels are in meters MSL.

Figure 2.4.6-219b Tsunami Water Level Contours 1.0 Hour into the Model Simulation



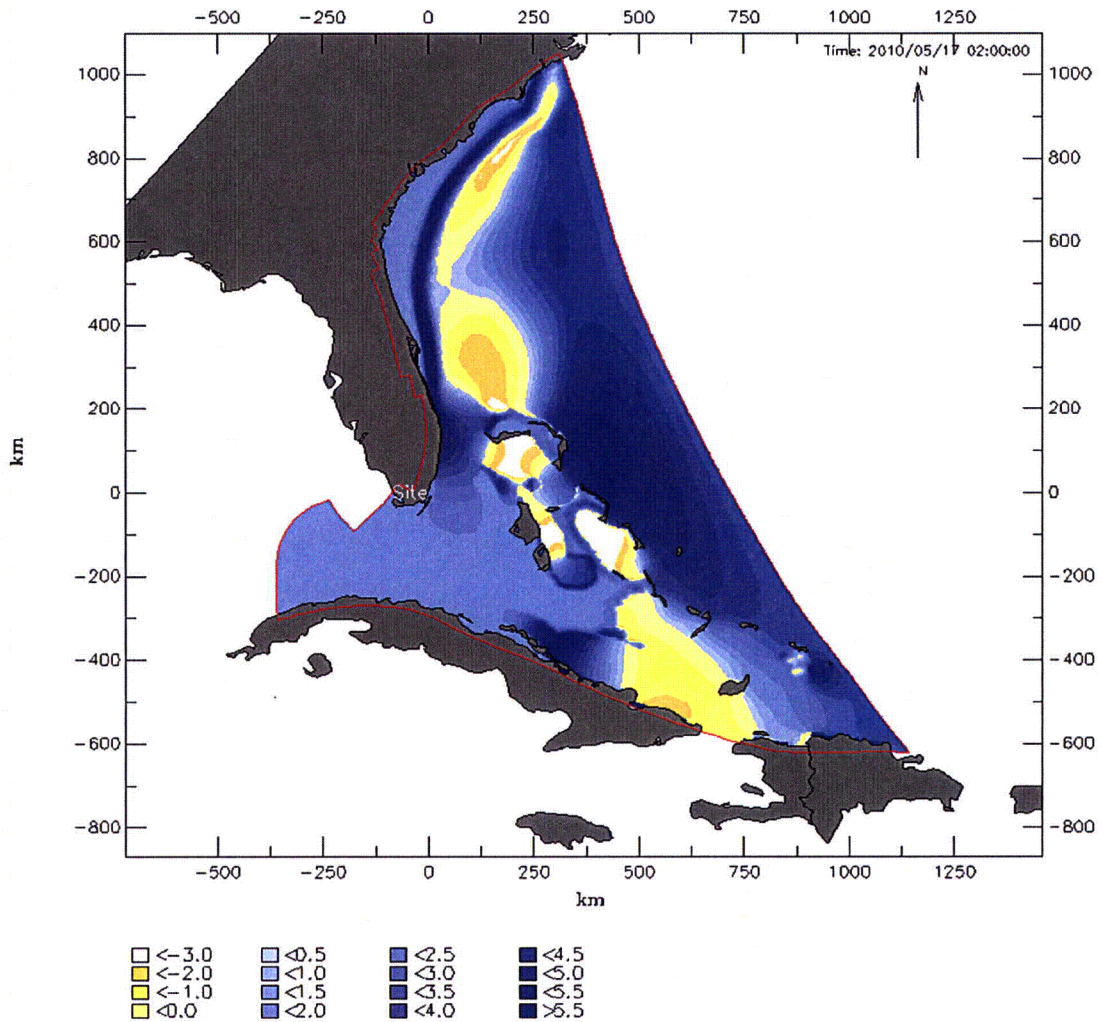
Note: Water levels are in meters MSL.

Figure 2.4.6-219c Tsunami Water Level Contours 1.5 Hours into the Model Simulation



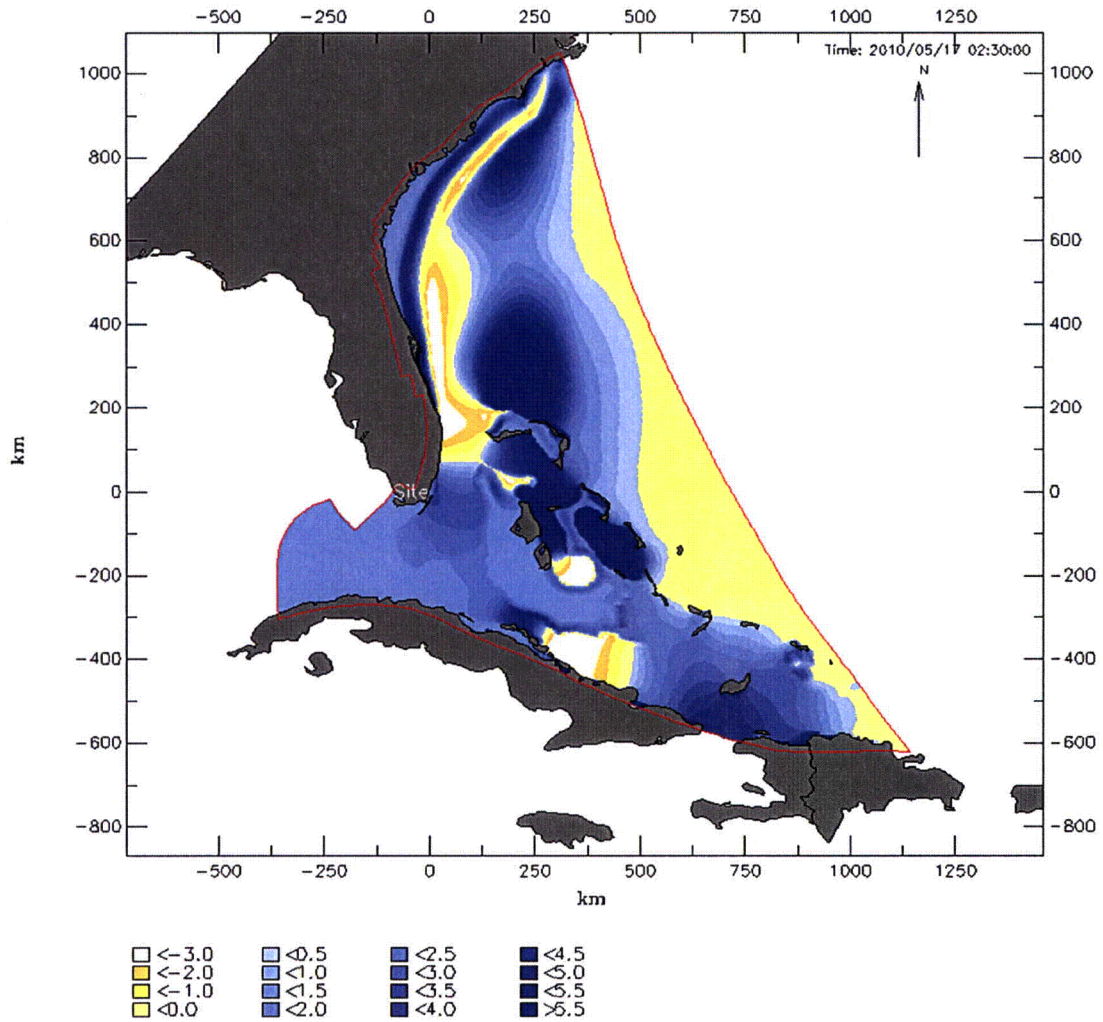
Note: Water levels are in meters MSL.

Figure 2.4.6-219d Tsunami Water Level Contours 2.0 Hours into the Model Simulation



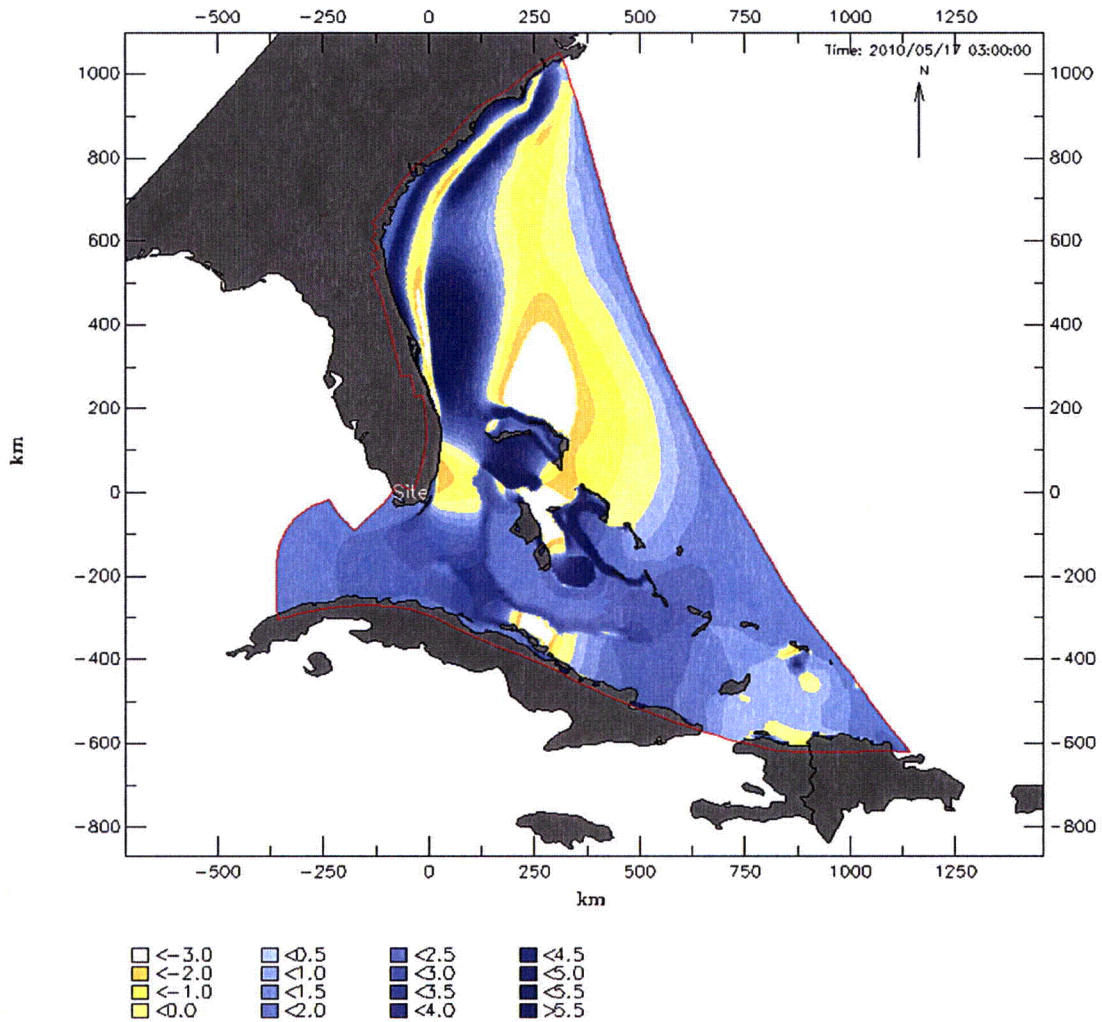
Note: Water levels are in meters MSL.

Figure 2.4.6-219e Tsunami Water Level Contours 2.5 Hours into the Model Simulation



Note: Water levels are in meters MSL.

Figure 2.4.6-219f Tsunami Water Level Contours 3.0 Hours into the Model Simulation



Note: Water levels are in meters MSL.

Figure 2.4.6-219g Tsunami Water Level Contours 3.5 Hours into the Model Simulation

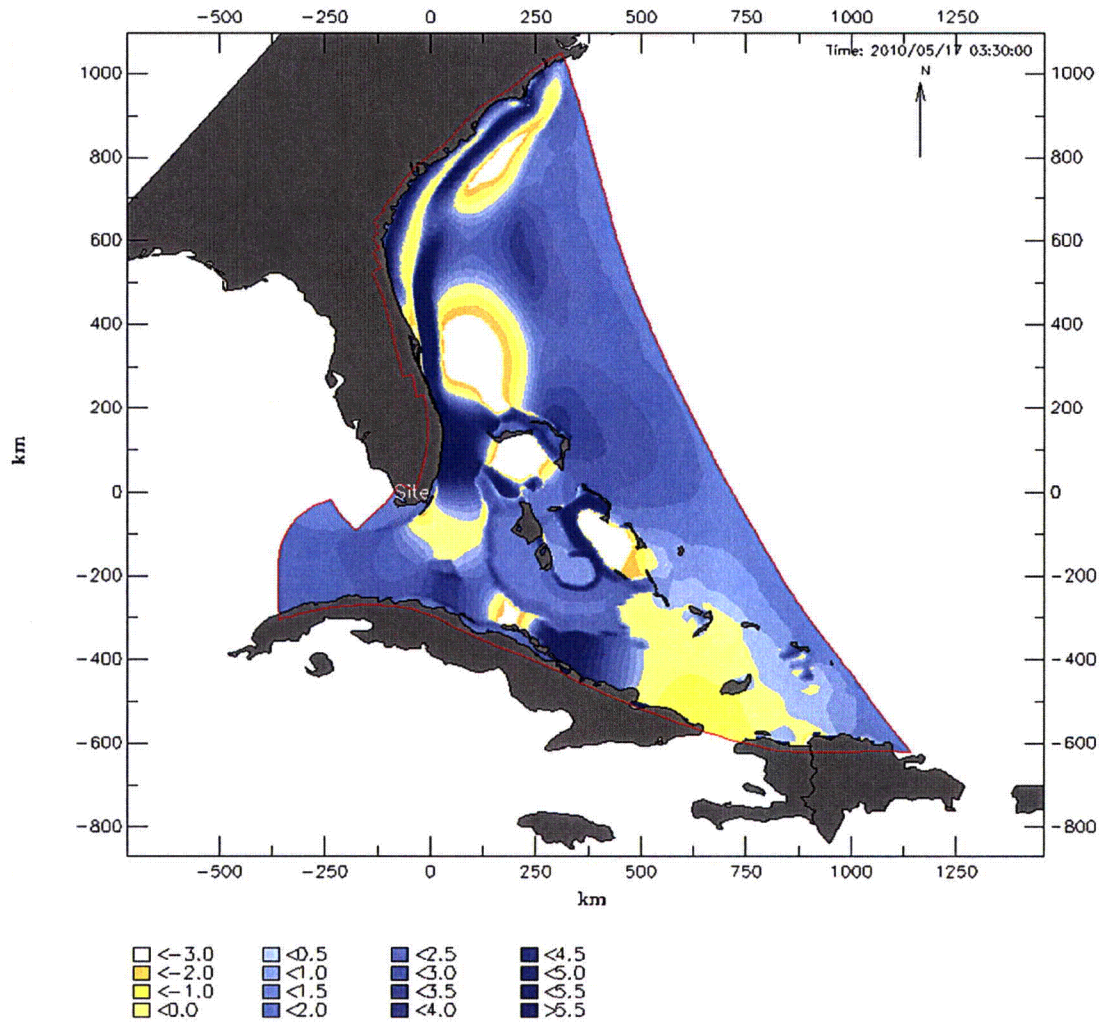
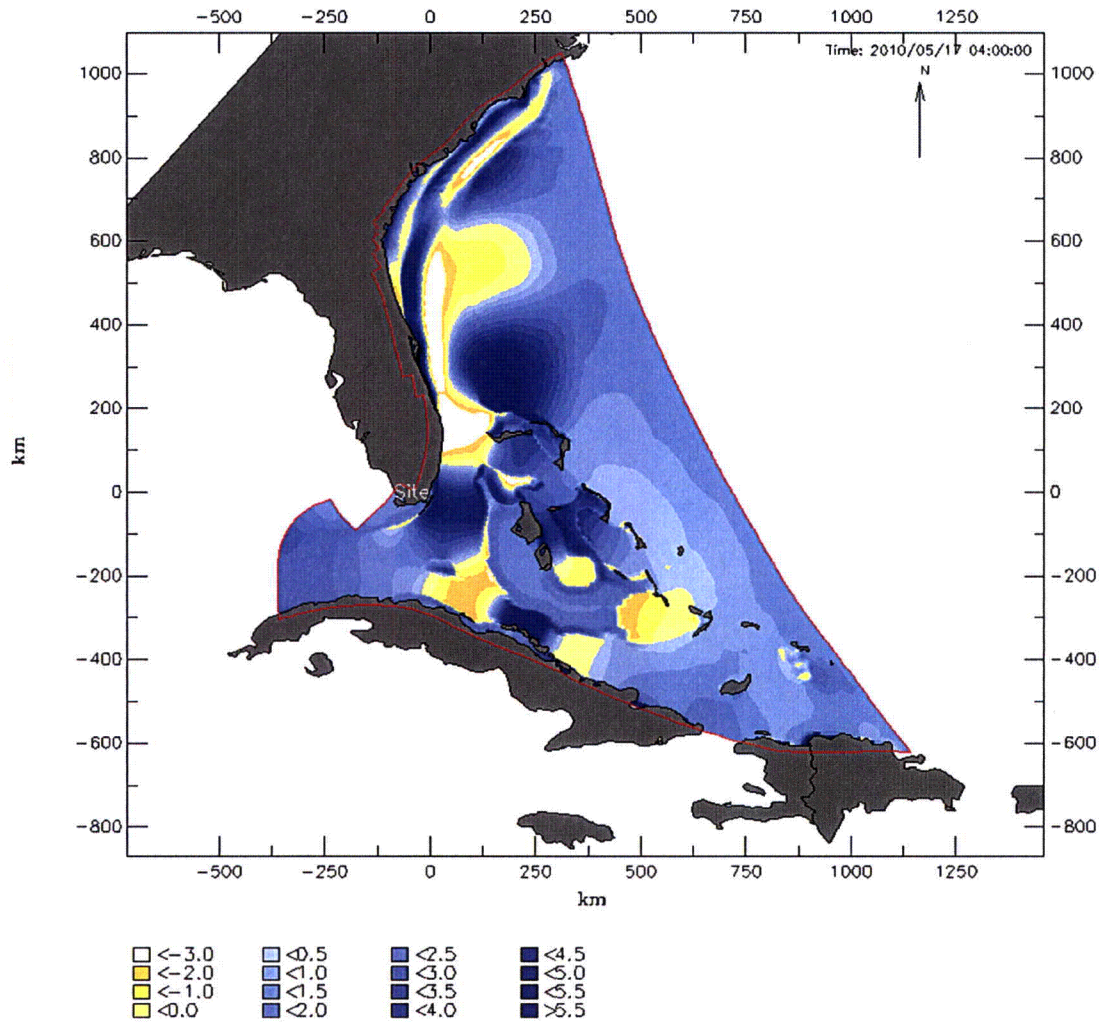
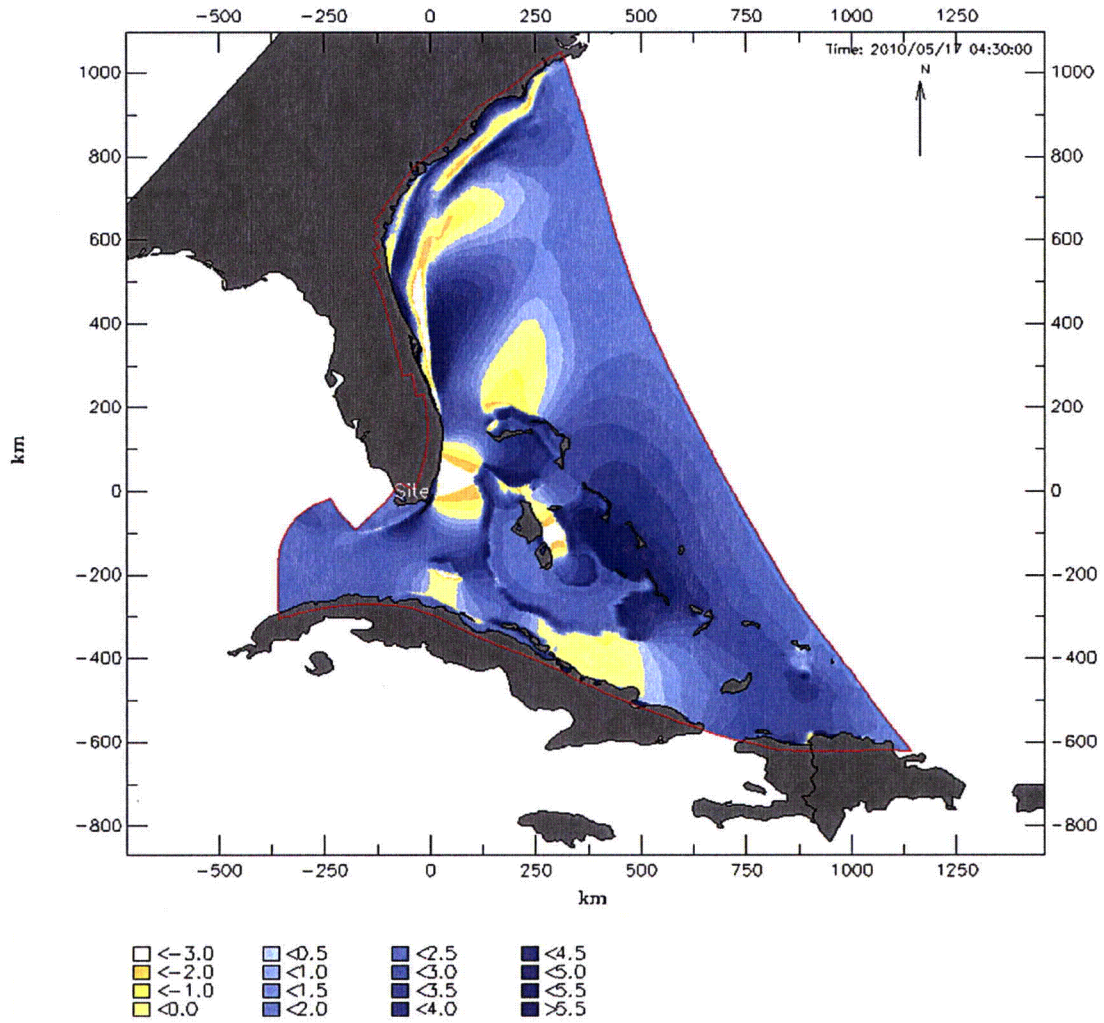


Figure 2.4.6-219h Tsunami Water Level Contours 4.0 Hours into the Model Simulation



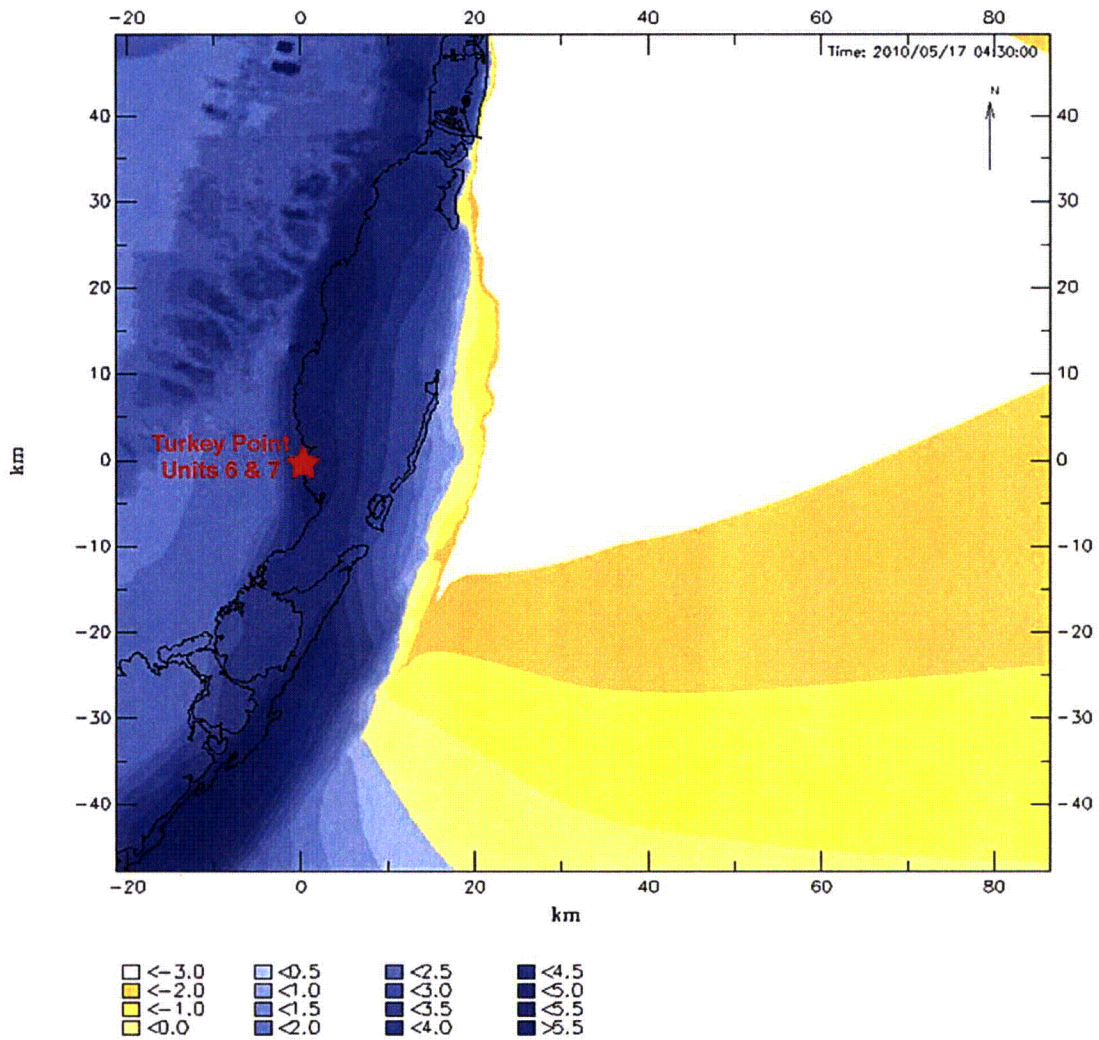
Note: Water levels are in meters MSL.

Figure 2.4.6-219i Tsunami Water Level Contours 4.5 Hours into the Model Simulation



Note: Water levels are in meters MSL.

Figure 2.4.6-220 Tsunami Water Level Contours near the Units 6 & 7 Site 4.5 Hours into the Model Simulation Corresponding to the Time Close to the Maximum Water Level at Site



Note: Water levels are in meters MSL; elevations shown for the inland area (dry cells) are ground elevations, not flood levels, according to designation in Delft3D-Flow.

Figure 2.4.6-221a Location of Simulated Water Level Monitoring Points along Track 1

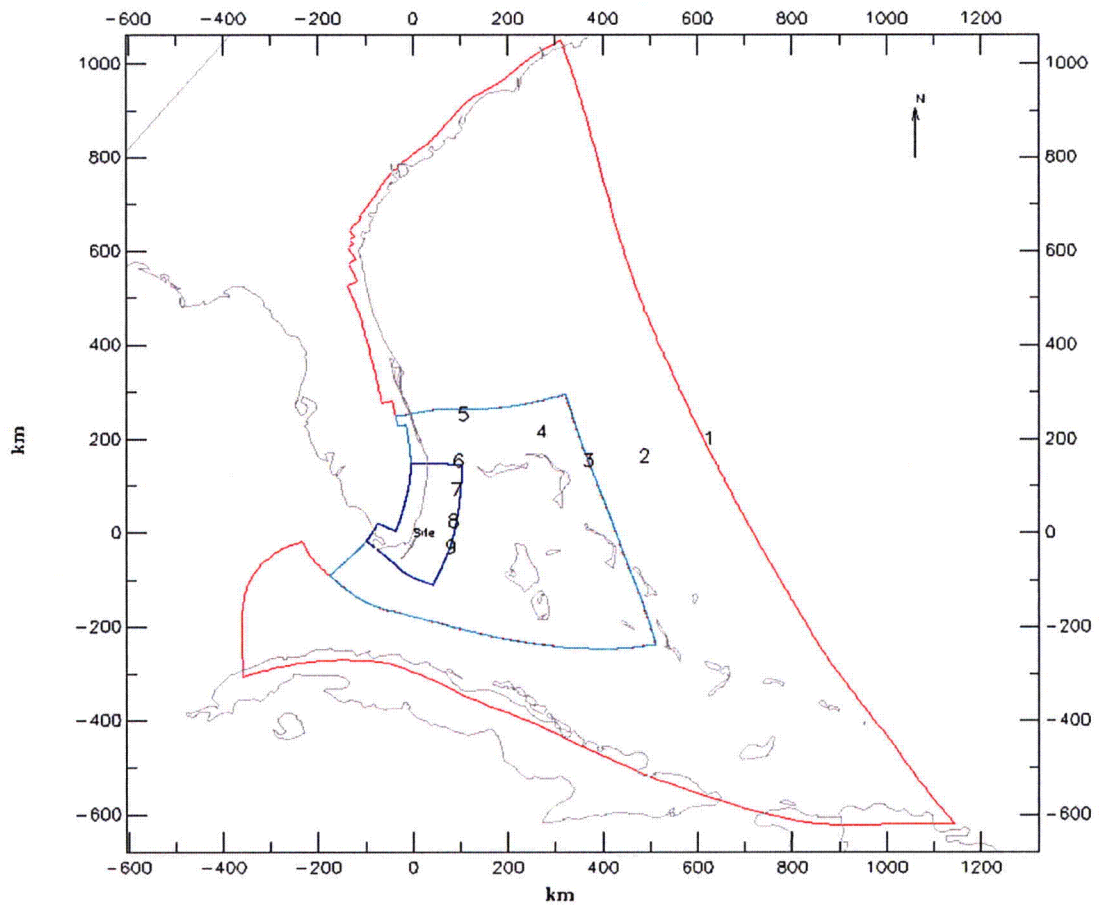


Figure 2.4.6-221b Location of Simulated Water Level Monitoring Points along Track 2

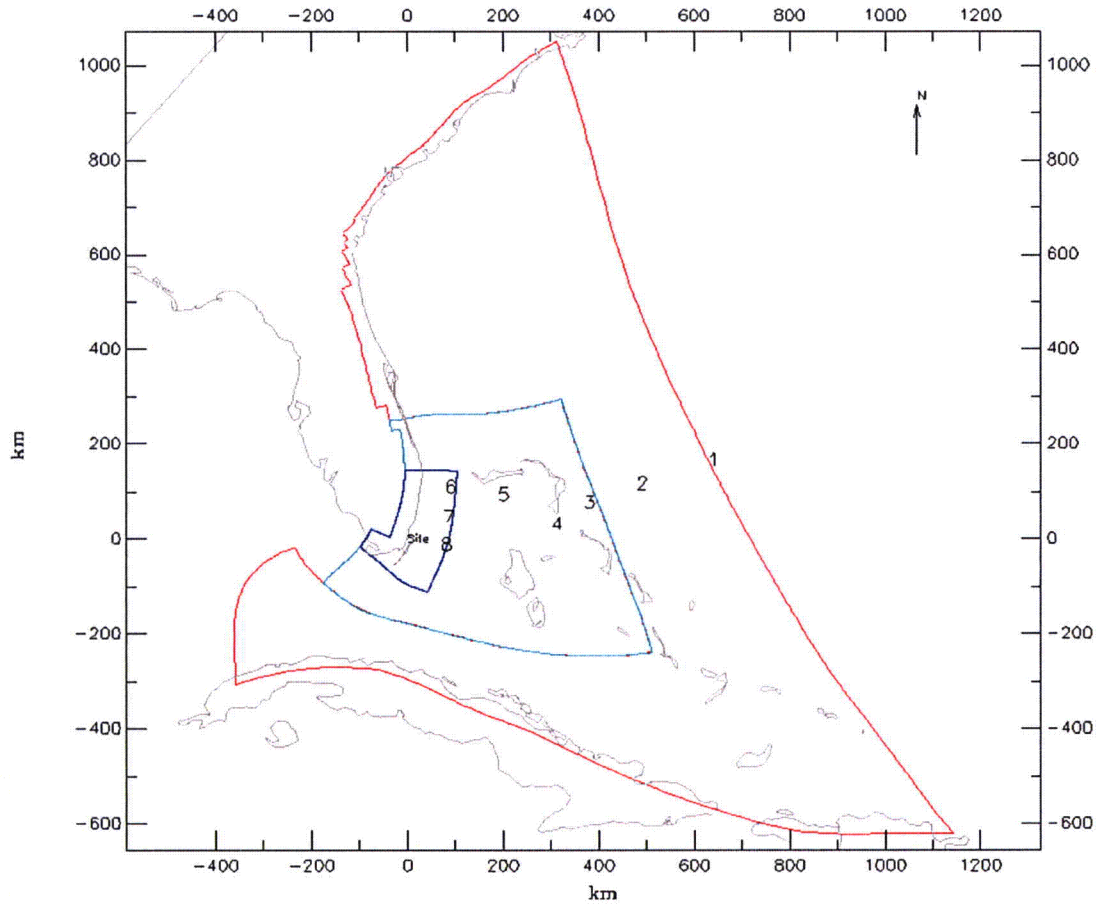


Figure 2.4.6-221c Location of Simulated Water Level Monitoring Points along Track 3

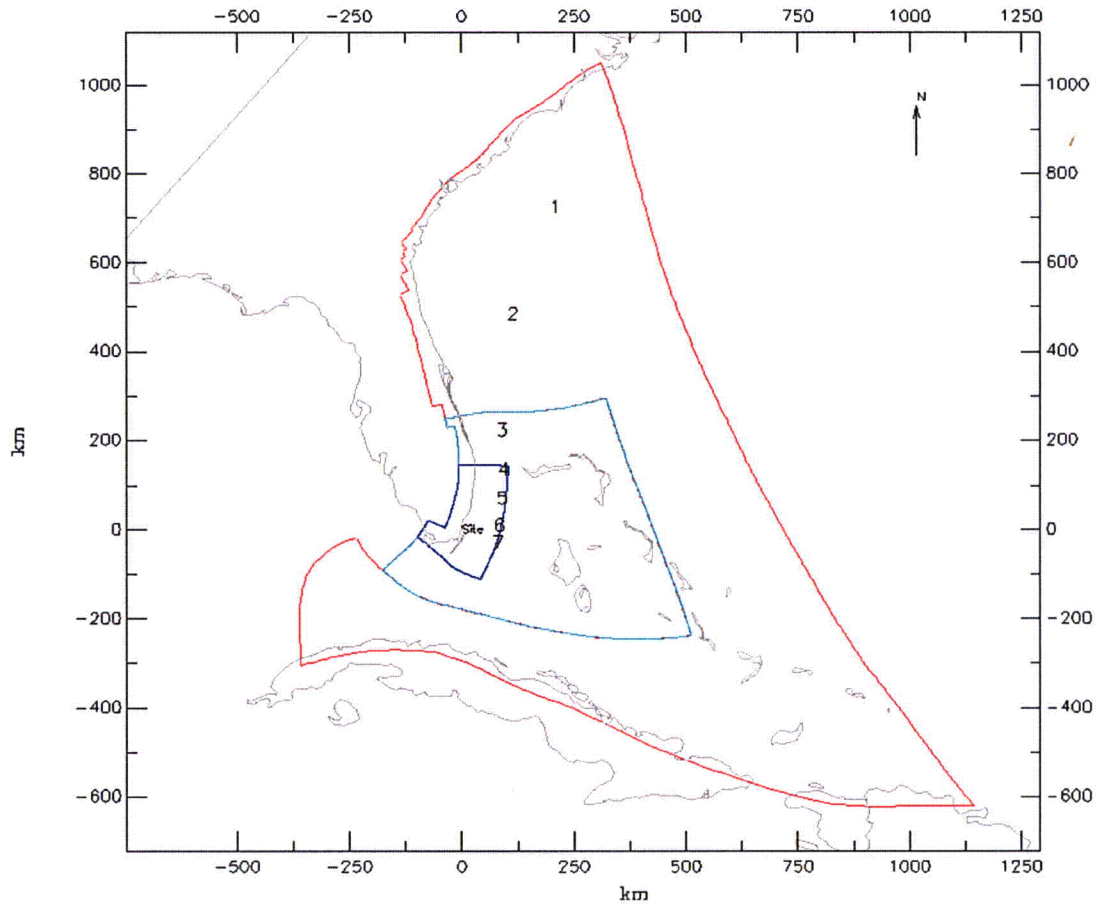
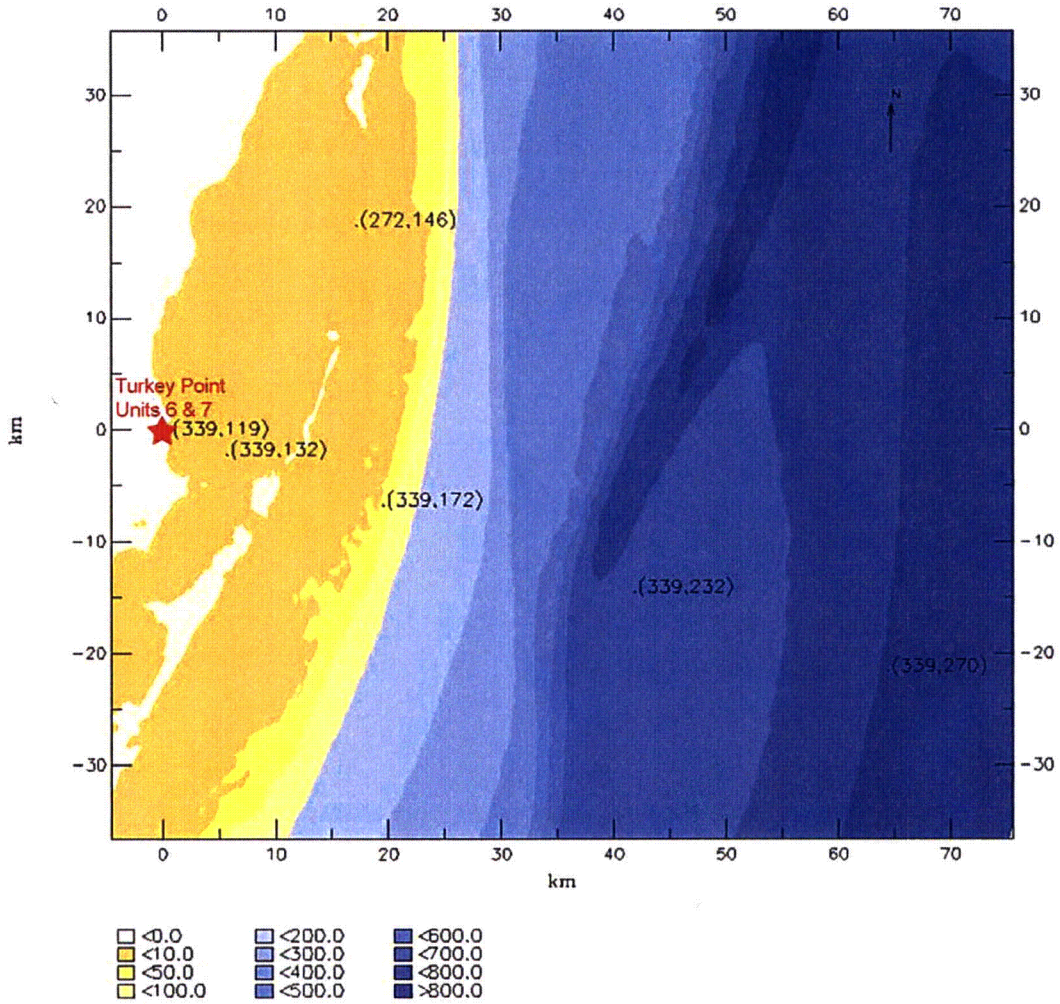


Figure 2.4.6-221d Location of Simulated Water Level Monitoring Points in Biscayne Bay and Vicinity (along with water depth contours)



Note: Depths to the seabed are in meters relative to MSL

Figure 2.4.6-222 Tsunami Marigrams at Monitoring Points along Track 1

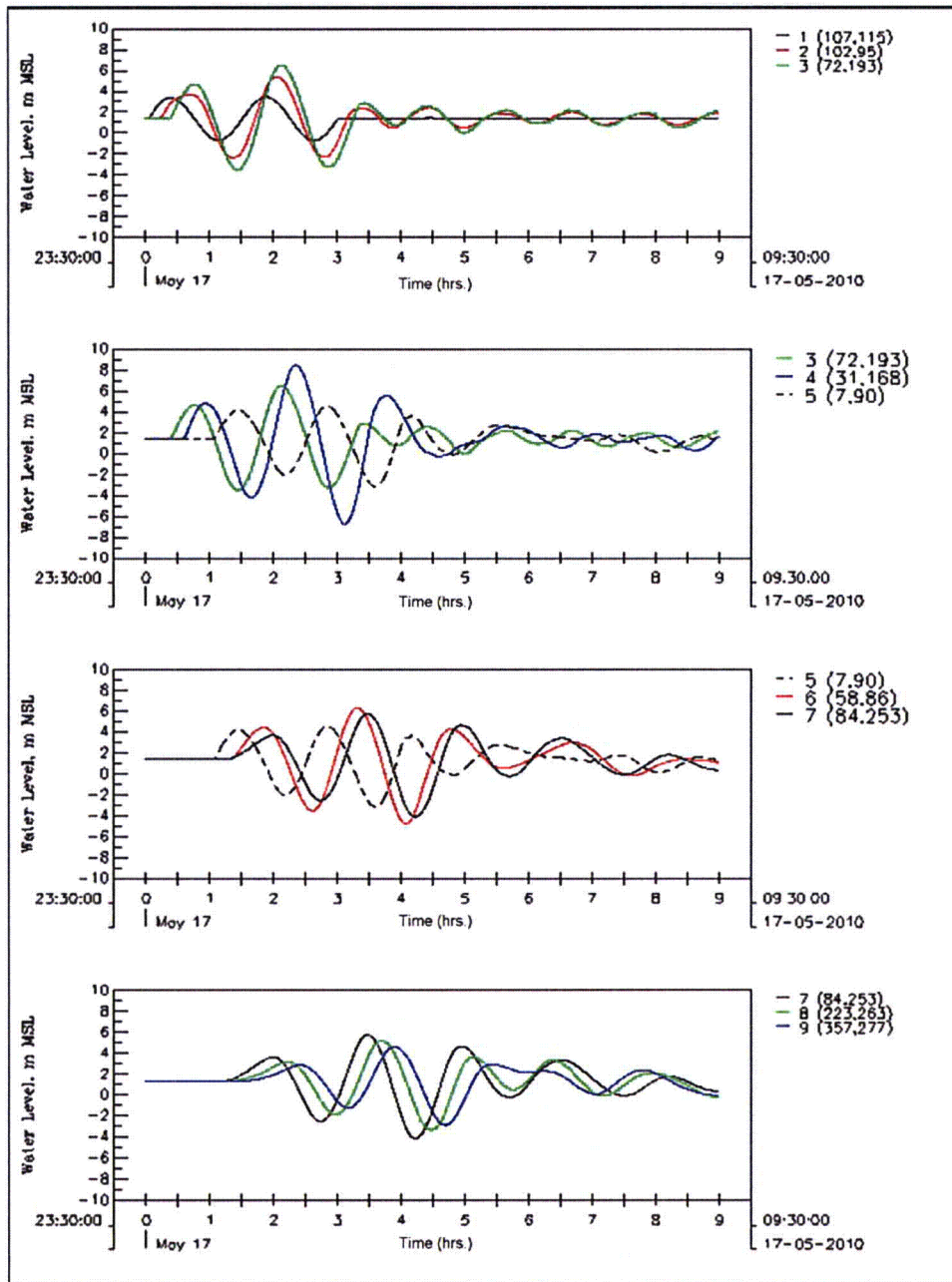


Figure 2.4.6-223 Tsunami Marigrams at Monitoring Points along Track 2

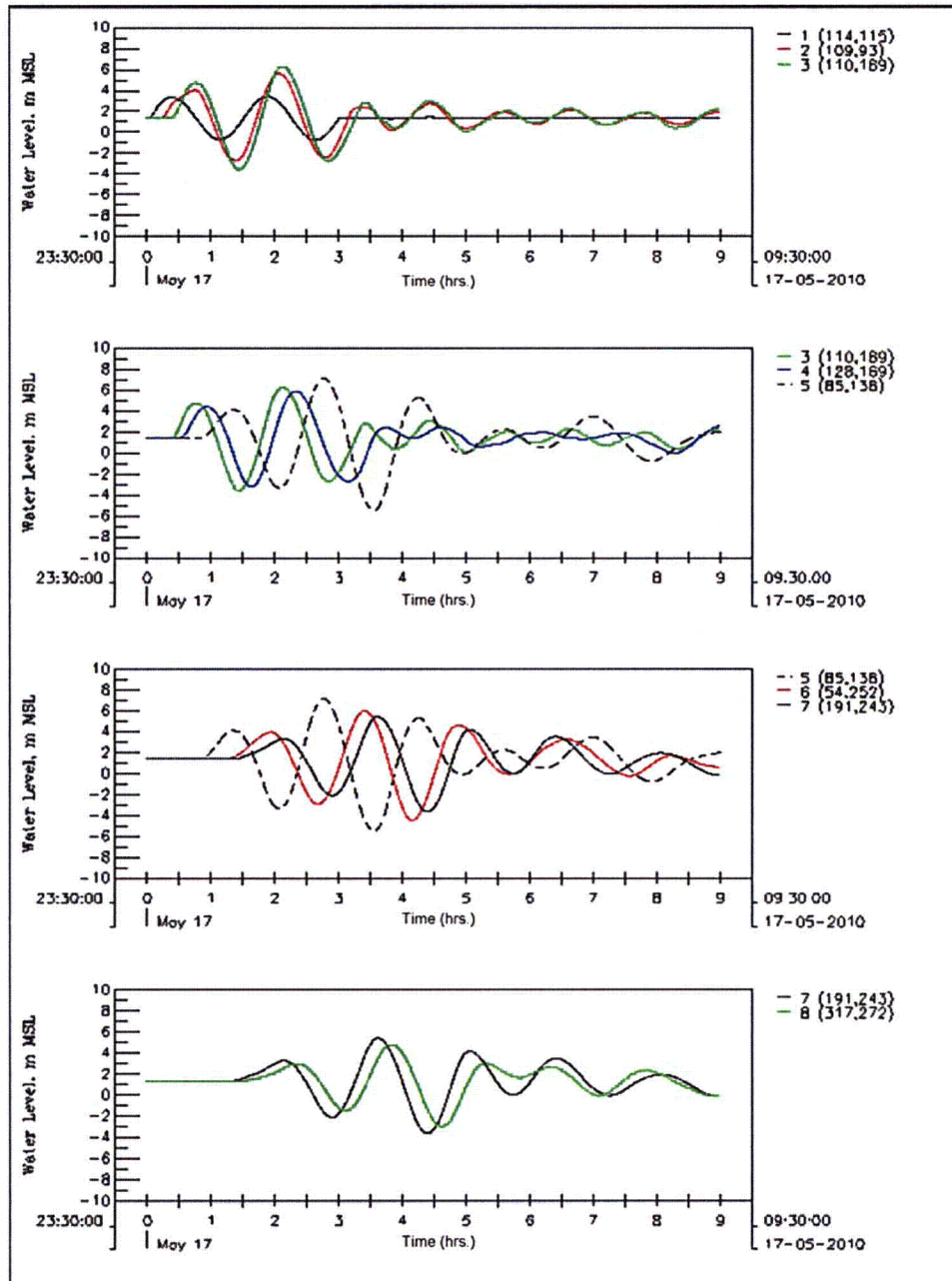


Figure 2.4.6-224 Tsunami Marigrams at Monitoring Points along Track 3

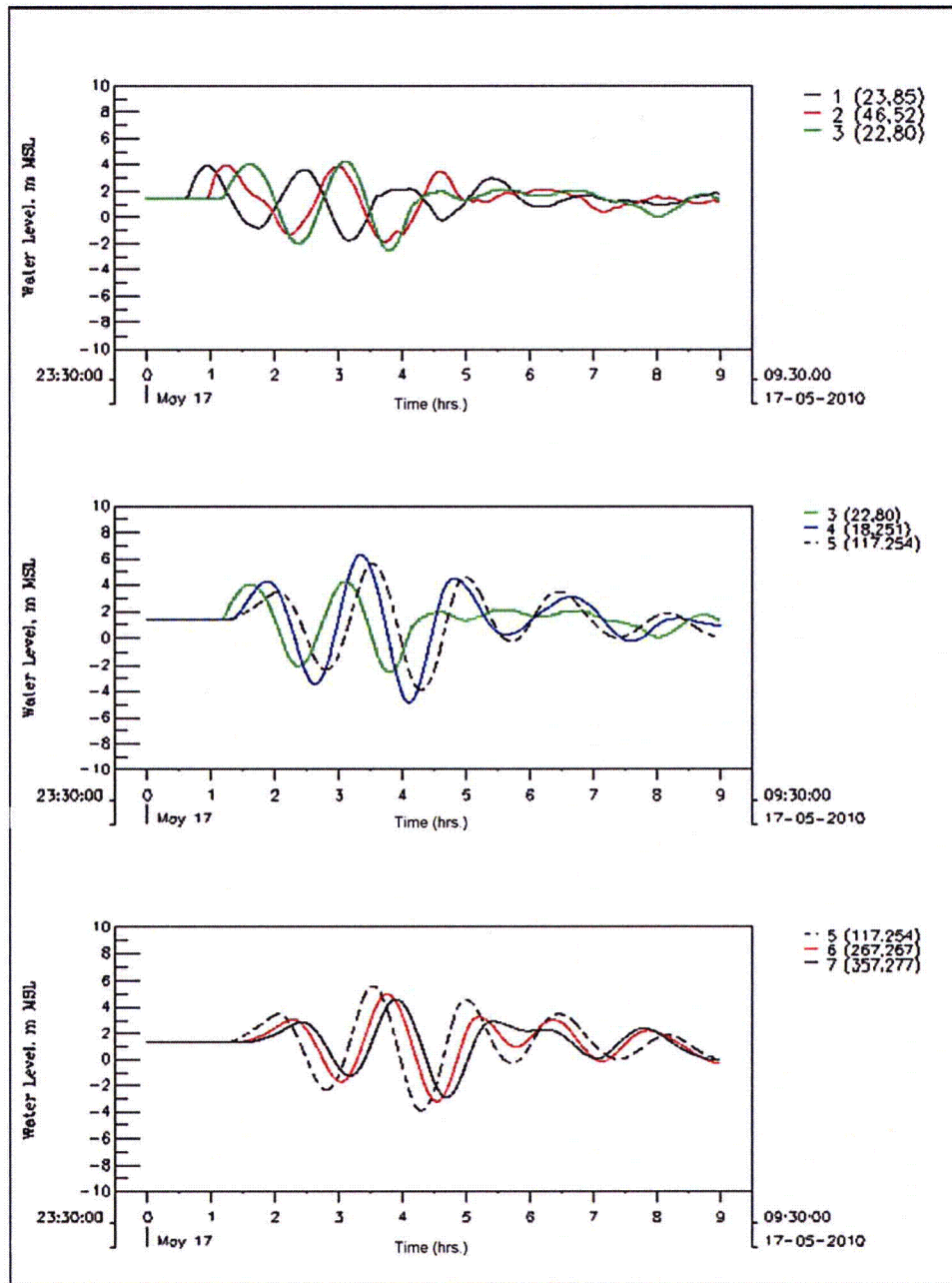


Figure 2.4.6-225 Tsunami Marigrams at Monitoring Points in Biscayne Bay and Vicinity

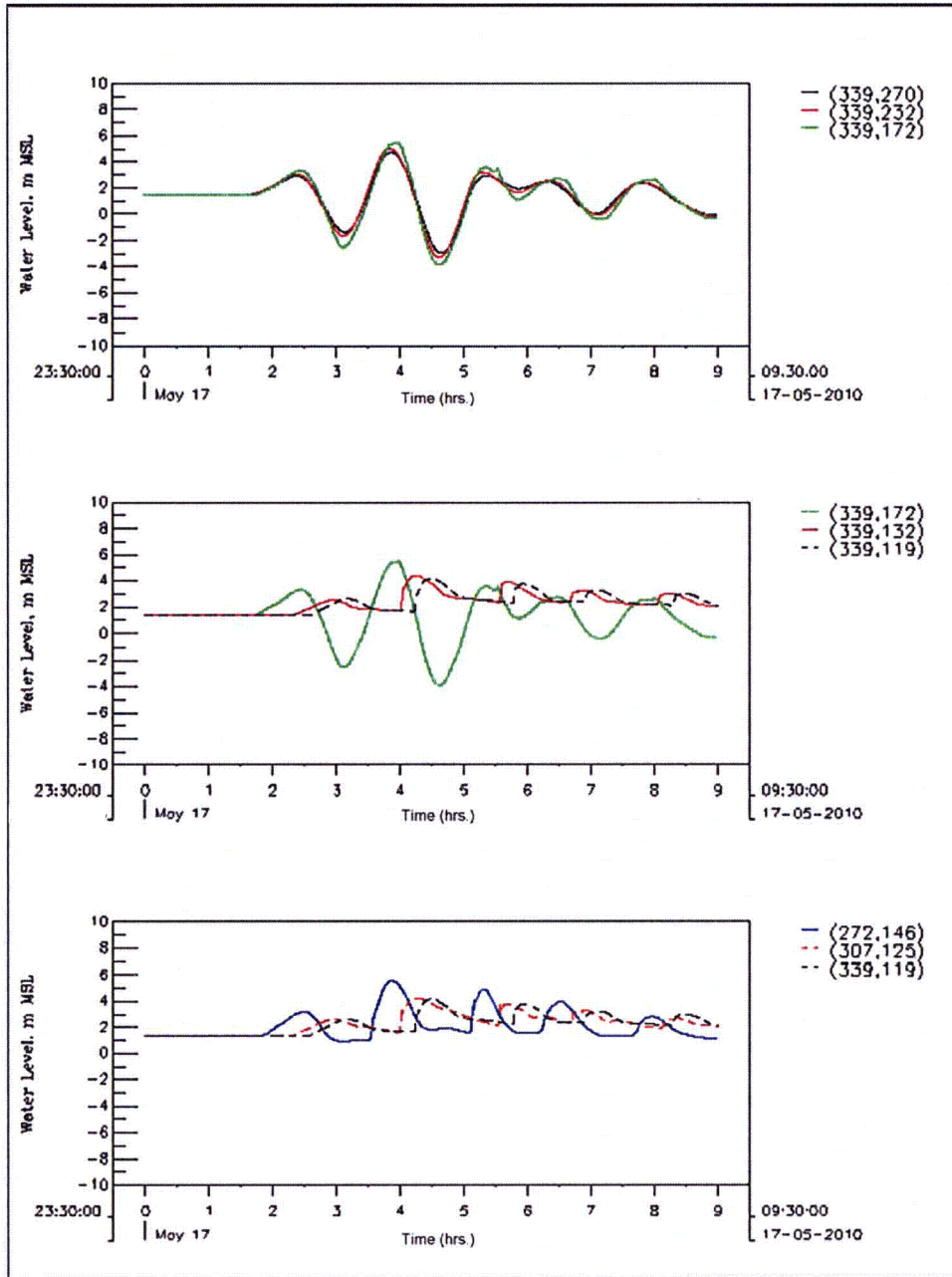
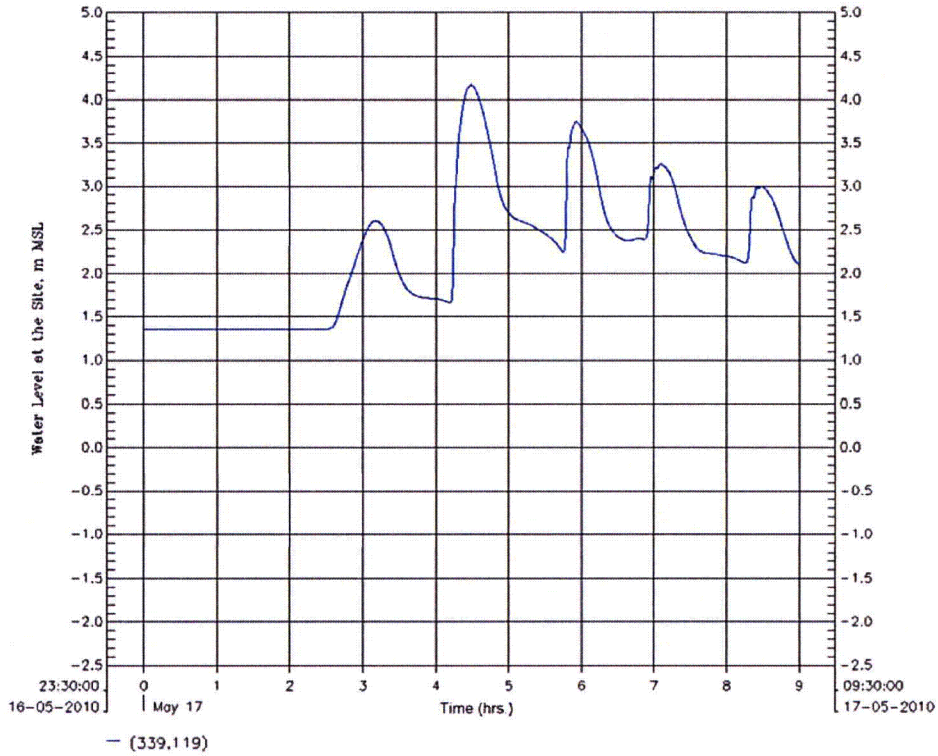


Figure 2.4.6-226 Simulated Tsunami Marigram at the Units 6 & 7 Site



Proposed Turkey Point Units 6 and 7
Docket Nos. 52-040 and 52-041
L-2010-215 Attachment Page 48 of 48

The fifth paragraph of Subsection 2.4.2.2 will be revised to reflect the updated maximum tsunami water level at the site in a future revision, as indicated below:

Subsection 2.4.6 describes the estimation of flood levels associated with the probable maximum tsunami (PMT). The maximum water level associated with the PMT at Units 6 & 7 is conservatively estimated to be ~~16.7~~**14.0** feet NAVD 88. Therefore, the PMT does not pose a flood risk to the safety-related facilities for Units 6 & 7.

ASSOCIATED ENCLOSURES:

None